2014

Understanding and improving microbial biofuel tolerance as a result of efflux pump expression through genetic engineering and mathematical modeling

William James Turner
University of Vermont

Understanding and improving microbial biofuel tolerance as a result of efflux pump expression through genetic engineering and mathematical modeling

A Thesis Presented

by

William J. Turner

to

The Faculty of the Graduate College

of

The University of Vermont

In Partial Fullfillment of the Requirements
for the Degree of Master of Science
Specializing in Mechanical Engineering

October, 2014

Accepted by the Faculty of the Graduate College, The University of Vermont, in partial fulfillment of the requirements for the degree of Master of Science in Mechanical Engineering.

Thesis Examination Committee:

Mary J. Dunlop, Ph.D. — Advisor

Jason Bates, Ph.D.

Yves Dubief, Ph.D.

Matt Wargo, Ph.D. — Chairperson

Cynthia J. Forehand, Ph.D. — Dean, Graduate College

Date: August 25, 2014

Abstract

Recent advances in synthetic biology have enabled the construction of non-native metabolic pathways for production of next-generation biofuels in microbes. One such biofuel is the jet-fuel precursor α-pinene, which can be processed into high-energy pinene dimers. However, accumulation of toxic biofuels in the growth medium limits the possible fuel yield. Overexpression of transporter proteins such as efflux pumps can increase tolerance to biofuels by pumping them out of the cell, thus improving fuel yields. However, too many efflux pumps can compromise the cell as well, creating a trade-off between biofuel toxicity and pump toxicity. In this work we improve the conditions of this trade-off in order to increase pinene tolerance in *E. coli*. We do so by constructing strains incorporating multiple efflux pumps from a variety of organisms and then testing them for tolerance in growth assay experiments. Previous research has suggested that certain combinations of efflux pumps can confer additional tolerance compared to the individual pumps themselves. However, the functional form of the combination of the tolerance provided by each pump and the toxicity due to their simultaneous activity is unknown. Using differential equations, we developed a growth model incorporating the trade-offs between toxicity of α-pinene and efflux pump activity to describe the dynamics of bacterial growth under these conditions. By analyzing biofuel toxicity and the effects of each efflux pump independently through a series of experiments and mathematical models, we propose a functional form for their combined effect on growth rate. We model the mean exponential growth rate as a function of pump induction and biofuel concentration and compare these results to experimental data. We also apply this technique to modeling toxicity of ionic liquids, a class of corrosive salts that has emerged as and effective chemical for pretreatment of biofuel production feedstock. We compare a model for a variety of ionic liquid responsive efflux pump controllers to that of an IPTG inducible controller and show agreement with experimental data, supporting the model's utility to test control schemes before conducting experiments. The overall goal of this project is to use modeling to guide design of tolerance mechanisms to improve overall biofuel yield.

Citations

Material from this Thesis has been submitted for review on July 11, 2014 in the following form:

Turner, W.J., Dunlop, M.J.. Trade-offs in Improving Biofuel Tolerance Using Combinations of Efflux Pumps. (In Review). 2014.

Material from this Thesis has been published in the following form:

Frederix M., Hütter K., Leu J., Batth T.S., Turner W.J., Thomas L. Rüegg, Blanch H.W., Simmons B. A., Adams P.D., Keasling J.D., Thelen M.P., Dunlop M.J., Petzold C. J., Mukhopadhyay A.. Development of a Native Escherichia coli Induction System for Ionic Liquid Tolerance. PLoS ONE 9(7). 2014.

Acknowledgements

Foremost, I would like to thank my advisor Prof. Mary Dunlop for her support, patience and guidance throughout the entirety of my research and thesis. Her enthusiasm and dedication to our work motivated me and made this project possible. I can not imagine a better advisor and mentor to have had throughout this process. I thank my thesis defense committee members, Doctors Jason Bates, Matt Wargo, and Yves Dubief, for contributing their ideas and guiding me throughout the proposal and defense. I would also like to thank my fellow labmates for their advice and assistance throughout my time as a researcher. Their opinions and suggestions have helped to shape this work and facilitated experimentation in the laboratory. Lastly, I would like to thank my family and girlfriend for their understanding and support in this important stage of my life.

This work was supported by The University of Vermont, the Office of Science (BER) at the U.S. Department of Energy and the NASA Vermont Space Grant Consortium.

Table of Contents

List of Figures

List of Tables

Chapter 1

Introduction

Literature review and introduction to concepts and modeling technique.

1.1 Background

Biofuel has sparked interest worldwide as an alternative source of transportation fuel that shows potential to provide a drop-in liquid alternative to modern petroleum products (13). Due to rising oil prices and political turmoil, nations are seeking a more sustainable fuel source that can provide them with the ability to produce their own fuel domestically while reducing the environmental impact of gasoline production. The ideal fuel must be highly energy dense and have minimal corrosive effect when burned in a modern combustion engine.

First generation biofuels, such as ethanol and biodiesel are already widely used, but they were selected mainly for convenience rather than their properties as fuels. The energy content of ethanol is only about 70% that of gasoline and it draws in moisture from the air at a higher rate, which increases corrosion in engines (13). Next generation biofuels are currently more costly to produce than ethanol but they can have higher energy content,

less corrosion, and higher octane numbers (resistance to knocking in spark-ignition engines). Isoprenoids are a class of biofuels that have favorable qualities due to branches and rings in the hydrocarbon chain that makes up their chemical structure (13). In this work we focus on the biofuel precursor α-pinene, a high energy content isoprenoid that can be processed into pinene dimers and used as a Jet-fuel replacement (7). Throughout this body of work we will refer to α-pinene and pinene interchangably.

Biofuel is produced by fermentation of feedstock made from a crop with high sugar content, usually cornflour in the US and sugarcane in Brazil. This competing land use issue presents a major limitation on biofuel production. However, waste cellulosic plant material from harvesting crops can be used as a fuel source, but this requires more effort to process into a fermentable sugar (4). The biomass must be processed into an easily digestible material for microbes. This can be achieved through a variety of mechanical and chemical processes such as milling and dissolution in strong acids, bases, alkanes or salts (10). Ionic liquids are strong salts that are liquid phase at room temperature. They have emerged as a viable solvent for pretreatment of biomass due to their chemical stability, which makes it possible to extract and reuse them after pretreatment (10). However, it is difficult to extract 100% of the ionic liquids that were originally used since they become homogenized with the feedstock.

In a microbial biofuel production process, bioengineered microbes are grown inside a reactor in a solution that is rich in cellulose-derived sugar (glucose and pentose). The chemical energy contained in the feedstock is converted by the microbe to a different molecular form through a metabolic pathway, where the end product is the desired biofuel. Accumulation of this biofuel in the cell's environment can be toxic (5). Figure 1.1 shows the toxicity of pinene to *Escherichia coli* (*E. coli*) when added extracellularly. When the growth medium becomes rich in fuel, fuel molecules penetrate diffusively and bind to the lipid bilayer of the cell membrane, affecting membrane fluidity and impairing functions such as transport

of vital but functionally unrelated compounds (15). Also, residual quantities of ionic liquid can make it into the reactor and inhibit microbial growth, limiting fuel yield (6). Thus, it is desirable to engineer strains that are tolerant to the biofuel product as well as pretreatment chemicals.

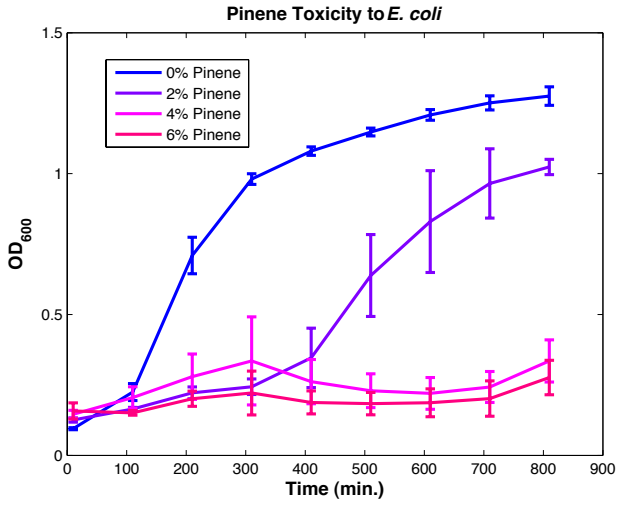

Figure 1.1: Pinene toxicity. Effect of increasing α-pinene concentration on growth of wildtype E. coli BW25113.

Efflux pumps are transporter proteins found in many cells and organisms that play a major role in the export of toxic compounds (11). There are numerous efflux pump genes in *E. coli* that target and transport a wide variety of molecules (11). Here, we focus on members of the resistance/nodulation/cell division (RND) family of efflux pumps. While many efflux pumps transport toxins through the inner membrane, RND efflux pumps transport a wide variety of biofuels and other antimicrobial chemicals across the inner and outer membranes using the electrochemical gradient across the membrane (12). It has been suggested that expression of multiple efflux pumps simultaneously can confer additional tolerance compared to the individual pumps (8). Due to the modularity enabled by modern synthetic biology techniques, the DNA for the metabolic pathway of particular fuels can be extracted from one organism and expressed heterologously in a host organism (1). In one

example, researchers constructed a production and efflux pathway in *E. coli* for the biofuel, limonene, using genes from 5 different organisms (3). The genes were assembled on plasmids and transformed into *E. coli*. An important conclusion from this study is that pumps that increase tolerance to the fuel can also increase yield. This was demonstrated by showing that an *E. coli* strain with a heterologous efflux pump from *Alcanivorax borkumensis* was able to produce significantly more limonene than a control strain without the pump.

The main efflux pump in *E. coli* is the AcrAB-TolC system, a tripartite protein complex that spans the inner and outer cell membrane and exports numerous chemicals such as antibiotics, solvents, detergents and dyes (12). AcrB is the inner membrane protein that is responsible for substrate recognition and export of toxic molecules. AcrA is the periplasmic linker that forms a connection to TolC, which is the outer membrane channel. TolC is the major outer membrane protein in *E. coli*, it works with a wide variety of inner membrane and periplasmic linker systems to transport everything from toxins to proteins (16).

Although efflux pumps provide an advantage in toxic environments, overexpression can compromise the cell membrane as well as consume metabolic energy that would otherwise be devoted to growth and replication processes, creating a trade-off scenario where expression must be finely balanced with toxicity of the environment to achieve optimum growth conditions (2). Figure 1.2 shows the toxicity of expressing the non-native efflux pump Pp_3456 from *Pseudomonas putida* in *E. coli*.

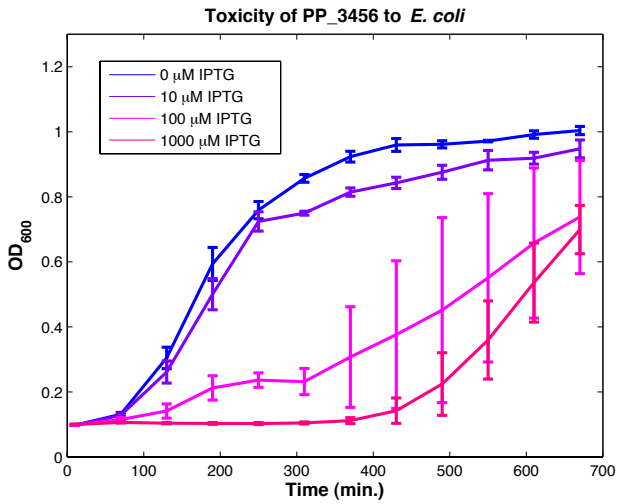

Figure 1.2: Toxicity of overexpression of the efflux pump Pp_3456 in E. coli. Pump protein genes are induced by IPTG.

1.2 Purpose

The objective of this thesis is to understand the trade-offs between toxicity (biofuel, pump, ionic liquid) and tolerance provided by efflux pumps. This was achieved through mathematical modeling and experiments investigating the of one and two efflux pumps in a controlled manner in order to understand how the tolerance and pump toxicity of the individual pumps and inhibitors combine. Efflux pumps were selected for their tolerance properties demonstrated in Dunlop *et al.* 2011 (3). Combinations of individual pumps were constructed and tested in *E. coli*. Mathematical models were developed and used to model the growth dynamics. Simulations are compared to experimental results and used to guide subsequent experiments with the goal of predicting modularity of efflux pumps based on individual pump data. This information will contribute to the long-term goal of improving fuel yields to make biofuels a more economically viable product.

1.3 Modeling Strategy

Bacterial growth is a complex process. Here we consider growth from a macro perspective where the total cellular mass increases with time based on the available nutrients. A bacterial growth curve generally consists of a lag phase, an exponential growth phase and a stationary growth phase, at which the cell density is considered steady-state. Jacques Monod proposed an empirical model for modeling bacterial growth in 1942 which he revised in 1949 (9). Monod's model (Eqn. 1.1 & 1.2) was the first growth model to introduce the concept of a limiting nutrient, which provides an elegant conversion of the growth substrate to biomass.

$$\dot{N} = \mu_{max} N \frac{S}{K_S + S} \tag{1.1}$$

N is the cell mass concentration, μ_{max} is the maximum growth rate, and S is the substrate concentration. K_s represents the half-saturation constant for the growth rate. Monod also found that the rate of nutrient consumption was opposite in sign and proportional to the growth rate. This leads to the equation for rate of change of limiting nutrient (Eqn. 1.2), where γ represents the growth yield.

$$\dot{S} = -\frac{1}{\gamma} \mu_{max} N \frac{S}{K_S + S} \tag{1.2}$$

In order to simulate inhibition of growth in the model, we modified the Monod model to include growth inhibition due to biofuel-specific effects. Equation 1.3 shows the modified form such that the growth rate decreases as the concentration of the inhibitory compound increases. The inhibition term is a ratio equal to 1 in the absence of the inhibitory compound, $C_i = 0$ g/L, and approaches zero as C_i approaches infinity, representing total inhibition. The inhibitor exponent, h, determines the curvature of the final cell density as a function of

the inhibitor concentration. K_c is the half-inhibition constant because when $C_i = K_c$, the inhibition ratio equals 0.5. Multiple inhibition terms can be included, each one representing an inhibitory compound such as a biofuel, ionic liquid, or pump protein.

$$\dot{N} = \mu_{max} N \frac{S}{K_S + S} \frac{1}{1 + (\frac{C_i}{K_c})^h} \tag{1.3}$$

The rate of efflux pump protein production, in other words transcription and translation of pump genes, depends on the type of genetic control governing their expression. Pump genes are always expressed at the basal level, α_{p0}, which depends on the particular gene and promoter. By selecting an appropriate promoter region for the pump gene, protein production can be activated at a static rate based on the concentration of an inducer molecule (Eqn. 1.4), or proteins can be controlled dynamically by the concentration of the inhibitor itself (2) (Eqn. 1.5) or any other metabolic compound for which a transcription factor is known. In Equation 1.5, α_p is the rate constant of protein production, and γ_I sets the expression threshold. Also, pump proteins degrade at the rate, β, proportional to their concentration.

$$\dot{P} = \alpha_{P0} + \alpha_p - \beta P \tag{1.4}$$

$$\dot{P} = \alpha_{P0} + \alpha_p \frac{C_i}{C_i + \gamma_p} - \beta P \tag{1.5}$$

P represents the pump protein concentration in the intracellular domain.The model accounts for passive diffusion of the toxic compound through the cell membrane. Taking the entire growth environment as the control volume,V_r, we can divide this control volume into two spaces: the intracellular volume V_i and the extracellular volume V_e. We assume that the total mass, m_r, of the toxic compound in the environment is constant (Eqn. 1.6). We also know that mass is equal to concentration multiplied by volume, we can use this to solve for the extracellular concentration as a function of the total, intra- and extracellular

volumes and intracellular concentration (Eqn. 1.7).

$$m_r = m_i + m_e \tag{1.6}$$

$$I_e = \frac{C_r V_r - C_i V_i}{V_e} \tag{1.7}$$

Cell mass was assumed to be 10^{-12}g, and cell volume was assumed to be 10^{-15}L (14). This balance rule is incorporated into the model upstream of the differential equations so that it is recalculated at each time-step with the other state variables. The inhibitory compounds diffuse passively through the cell membranes at a rate dependent on the gradient of concentrations on either side of the membrane (Eqn. 1.8).

$$\frac{dC_i}{dt} = \alpha_c 0 \frac{V_e}{V_i}(C_e - C_i) - C_i \alpha_c P \tag{1.8}$$

The gradient is multiplied by a rate constant and the change in concentration due to mass flux is accounted for by the volume ratio between the intracellular and extracellular environments. Inhibitory compounds are also actively transported out of the intracellular environment at a rate proportional to the efflux pump concentration. We assume the inhibitor only impacts growth when in the intracellular environment, therefore the pumps provide an advantage by transporting the compounds out of the cell. As an example, Figure 3 shows simulated growth curves and the toxicity profile for a range of hypothetical inhibitor concentrations. The dimensionless quantity $N/\gamma K_s$ is plotted in order to show a typical growth curve while maintaining generality for all units and measures of bacterial population density. No efflux pumps are active in this simulation.

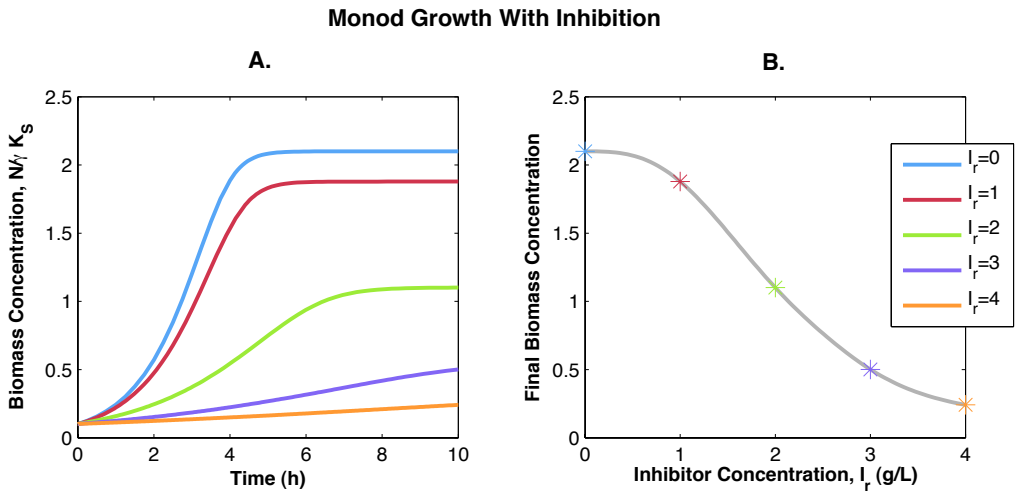

Figure 1.3: Simulated growth curves (a) and toxicity profile (b) for a range of inhibitor concentrations and typical constants for E. coli. Parameters: $r = 1.35/h$, $K_s = 0.004\ g/L$, $\gamma_m = 0.23$, $n = 3$, $K_c = 2\ g/L$. *Initial conditions:* $N_0 = 0.1/\gamma K_S$, $S_0 = 2K_S$. *The stars in (b) are the end values of the simulation in (a), the grey curve shows the same result for a higher resolution of inhibitor concentrations.*

Bibliography

[1] Atsumi, S., T. Hanai, and J. C. Liao. Non-fermentative pathways for synthesis of branched-chain higher alcohols as biofuels. Nature 451, 86 to 89. (2008).

[2] Dunlop, Mary J., Jay D. Keasling, and Aindrila Mukhopadhyay. A model for improving microbial biofuel production using a synthetic feedback loop. Systems and synthetic biology 4.2, 95-104. (2010).

[3] Dunlop, Mary J., Zain Y. Dossani, Heather L. Szmidt, Hou Cheng Chu, Taek Soon Lee, Jay D. Keasling, Masood Z. Hadi, and Aindrila Mukhopadhyay. Engineering microbial biofuel tolerance and export using efflux pumps. Molecular systems biology 7, no. 1. (2011).

[4] Fargione, Joseph, Jason Hill, David Tilman, Stephen Polasky, and Peter Hawthorne. Land clearing and the biofuel carbon debt. Science 319, no. 5867, 1235-1238. (2008).

[5] Fischer, Curt R., Daniel Klein-Marcuschamer, and Gregory Stephanopoulos. Selection and optimization of microbial hosts for biofuels production. Metabolic engineering 10.6, 295-304. (2008).

[6] Frederix, M., K. Hutter, J. Leu, T. S. Bath, W. J. Turner, T. L. Rüegg, H. W. Blanch, B. D. Simmons, P. D. Adams, J. D. Keasling, M. P. Thelen, M. J. Dunlop, C. J. Petzold, A. Mukhopadhyay. Development of a Native *Escherichia coli* Induction System for Ionic Liquid Tolerance. PloS one, 9(7), e101115. (2014).

[7] Harvey, Benjamin G., Michael E. Wright, and Roxanne L. Quintana. High-density renewable fuels based on the selective dimerization of pinenes. Energy & Fuels 24.1, 267-273. (2009).

[8] Lee, Angela, Weimin Mao, Mark S. Warren, Anita Mistry, Kazuki Hoshino, Ryo Okumura, Hiroko Ishida, and Olga Lomovskaya. Interplay between efflux pumps may provide either additive or multiplicative effects on drug resistance. Journal of bacteriology 182, no. 11, 3142-3150. (2000).

[9] Jacques Monod. The growth of bacterial cultures. Annual Reviews in Microbiology. (1949).

[10] Mora-Pale, Mauricio, Luciana Meli, Thomas V. Doherty, Robert J. Linhardt, and Jonathan S. Dordick. Room temperature ionic liquids as emerging solvents for the pretreatment of lignocellulosic biomass. Biotechnology and bioengineering 108, no. 6, 1229-1245. (2011).

[11] Nikaido, Hiroshi. Multidrug efflux pumps of gram-negative bacteria. Journal of Bacteriology 178.20, 5853. (1996).

[12] Paulsen, Ian T. Multidrug efflux pumps and resistance: regulation and evolution. Current opinion in microbiology 6.5, 446-451. (2003).

[13] Peralta-Yahya, Pamela P., Fuzhong Zhang, Stephen B. Del Cardayre, and Jay D. Keasling. Microbial engineering for the production of advanced biofuels. Nature 488, no. 7411, 320-328. (2012).

[14] Phillips, R., Kondev, J., Theriot, J., & Garcia, H.. Physical biology of the cell (pp. 281-321). New York: Garland Science. (2009).

[15] Ramos, Juan L., Estrella Duque, MaríaTrinidad Gallegos, Patricia Godoy, María Isabel Ramos-González, Antonia Rojas, Wilson Terán, and Ana Segura. Mechanisms of solvent tolerance in gram-negative bacteria. Annual Reviews in Microbiology 56, no. 1, 743 to 768 (2002).

[16] Rosner, Judah L., and Robert G. Martin. Reduction of Cellular Stress by TolC- Dependent Efflux Pumps in *Escherichia coli* Indicated by BaeSR and CpxARP Activation of spy in Efflux Mutants. Journal of bacteriology 195.5, 1042-1050. (2013).

[17] Rüegg, T. L., Kim, E. M., Simmons, B. A., Keasling, J. D., Singer, S. W., Lee, T. S., & Thelen, M. P. An auto-inducible mechanism for ionic liquid resistance in microbial biofuel production. Nature communications, 5. (2014).

Chapter 2

Trade-offs in Improving Biofuel Tolerance Using Combinations of Efflux Pumps

The following chapter contains materials under review for publication.

2.1 Introduction

Microbial production of next-generation biofuels has the potential to provide drop-in alternatives to liquid petroleum products including gasolines, diesels, and jet fuels (21). Aviation fuels, in particular, represent an area where biofuels are especially important. In contrast to other transportation markets that have alternative renewable technologies (e.g. gasoline vs. electric vehicles), aviation requires liquid fuels that are energy dense, work at low temperatures, and are not prohibitively expensive. Terpenes are naturally occurring compounds in plant biochemistry that have the potential to serve as next-generation jet fuels. Several studies have engineered pathways for terpene production in microbial hosts (1, 24, 32). Recently, pinene has been synthesized as a jet fuel replacement (1, 24). Pinene dimers have a similar heating value and energy density to the tactical jet fuel JP-10 and can be readily synthesized from α-pinene by chemical catalysis (24, 13).

2.1. INTRODUCTION

Although they hold great promise as renewable jet fuels, end product inhibition is a critical factor in the microbial synthesis of monoterpenes (24, 2). Therefore, as biofuel production improves, it will be necessary to also improve host tolerance. As the intracellular concentration of biofuel increases, the protective barrier provided by the cell membrane is weakened and membrane permeability and fluidity increase from the breakdown of the tightly packed lipid bilayer. As a result, cellular machinery and energy can be released across the membrane in the form of ions, ATP, RNA, and proteins. This impacts electrochemical energy gradients such as the proton motive force that normally provide the driving force for essential transport processes (7, 26).

Microbes have evolved a wide variety of mechanisms to combat the effects of solvent toxicity (20, 22). These include alteration in the membrane phospholipid composition for reduced permeability, active extrusion by efflux pumps, and heat shock protein assistance in the refolding of unraveled proteins (7, 20). Here, we focus on the transport of solvents by efflux pumps. Several previous studies have demonstrated that expression of pumps can improve biofuel production (6, 9, 28). There is evidence that combinations of efflux pumps can confer additional tolerance compared to expression of either pump individually (16). Notably, bacteria have evolved to have multiple parallel efflux pump systems. In *P. putida* DOT-T1E, toluene tolerance is achieved by three solvent resistant pumps, collectively known as the toluene tolerance genes (*ttg*), which work in concert to improve tolerance (23). Here, we asked whether simultaneous heterologous expression of non-native efflux pumps in *E. coli* could enhance pinene tolerance relative to a wildtype control and strains containing individual pumps.

Overexpression of efflux pumps can be detrimental to growth, due to an overloading of membrane insertion machinery and changes in membrane composition (20, 29). This creates a trade-off between pump toxicity and biofuel toxicity where moderate, but not high, expression is necessary to achieve optimal growth (5, 12). Similar trade-offs have

been observed with efflux pumps in antibiotic resistance(30). With combinations of pumps there are multiple sources of pump toxicity, but also potential combinatorial benefits from reduced biofuel toxicity. Balancing these competing factors has the potential to introduce a complex fitness landscape. In addition, testing combinations of pumps under different induction conditions with different levels of biofuel quickly results in a large set of conditions requiring experimental characterization. Here, we show experimentally that a simple model of toxicities is sufficient to predict how two pumps act in concert, greatly reducing the number of validation experiments required.

In this study, we used four efflux pumps that are known to improve tolerance to α-pinene (6). Here, we refer to the pumps by the gene numbers of the inner membrane component, however we note that each pump is composed of multiple genes (Methods). Pp_3456 is native to *Pseudomonas putida* KT2440, Maqu_3494 and Maqu_0582 are from *Marinobacter aquaeolei*, and Abo_0964 is from *Alcanivorax borkumensis* SK2. *P. putida* is a soil bacterium with known solvent tolerance properties (19), *M. aquaeolei* is a hydrocarbon degrader that was isolated from the head of an offshore oil well (14, 27), and *A. borkumensis* is known to dominate hydrocarbon-rich marine environments like those near natural oil seepages or oil spills (25, 31). When tested individually in a strain of *E. coli* lacking the major native solvent-tolerance pump, all four pumps were shown to improve pinene tolerance (6). In the present study, we comprehensively characterized the biofuel and pump toxicities for each pump individually and then combined pumps, repeating tolerance experiments. Using the single pump experimental data, we fit a mathematical model describing the cell growth. From the single pump data we were able to accurately predict the fitness landscape with multiple pumps using the mathematical model. This result shows excellent agreement with all tested combinations of pump induction and biofuel levels. Importantly, this suggests that a small number of experiments may be sufficient to predict combinatorial effects between pumps.

2.2 Results and discussion

In order to quantify the benefit of efflux pump expression and the toxicity of each pump, we performed growth assays with a gradient of pinene concentrations and different levels of pump induction (Methods). Because we were interested in testing how combinations of pumps impacted growth, we used a two plasmid system in all experiments. Using *E. coli* BW25113 as a host, we cotransformed cells with compatible medium copy (p15A origin) and low copy (SC101 origin) plasmids (Methods). As a negative control, we expressed red fluorescent protein (*rfp*) and compared this to expression of each efflux pump, individually or in combination. For concise notation, we refer to the medium copy plasmid (p15A) as A and the low copy plasmid (SC101) as S. For example, A-*rfp*/S-*rfp* is the negative control, expressing no non-native efflux pumps, and A-Maqu_3494/S-*rfp* is a single pump strain, with Maqu_3494 expressed from the medium copy plasmid.

In the wildtype strain, we observed a severe growth impact with 0.5% and 1% pinene (Fig. 2.1a). Although the pinene levels tested here are well above those produced in engineered strains at present (e.g. 0.004%, or 32 mg/L in E. coli (24)), improving tolerance can increase yields even when the biofuels being produced are well below toxic levels (6). We next expressed Maqu_3494 under the control of the lacUV5 promoter and induced cultures with 10 μM IPTG, resulting in low-to-moderate induction of the pump. The strain harboring the pump was able to partially restore growth in the presence of 0.5% and 1% pinene (Fig. 2.1b). Next, we measured the impact of pump toxicity by adjusting the level of IPTG induction in the absence of pinene. Figure 2.1c shows the effect of Maqu_3494 overexpression on growth. As the inducer concentration is increased, the cells grow more slowly. These data show the independent effects of biofuel and pump toxicity, suggesting a trade-off when optimizing efflux pump expression.

To interpret the combined effects of these two phenomena, we used the experimental

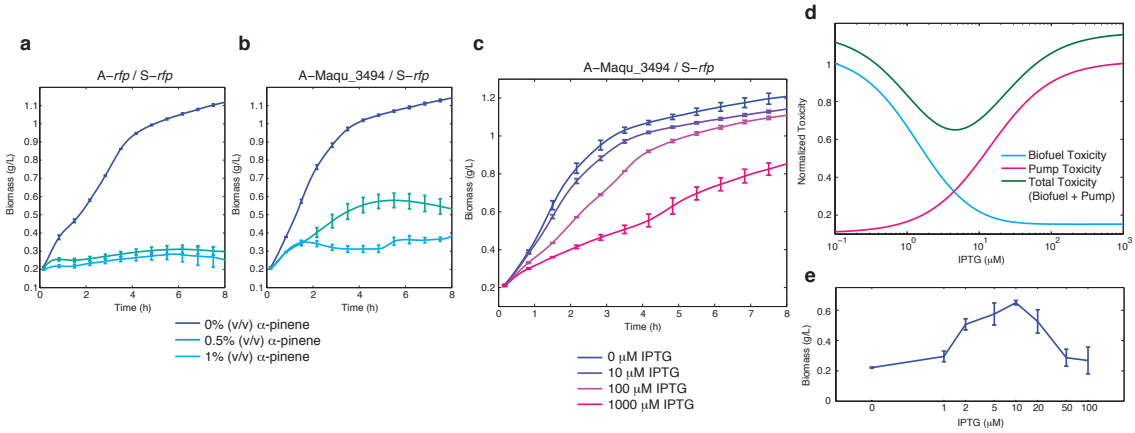

Figure 2.1: Costs and benefits of efflux pump expression. (a) IPTG-induced expression of the negative control, E. coli BW25113 with plasmids A-rfp/S-rfp, exhibits pinene toxicity. (b) Induction of a single pump strain A-Maqu_3494/S-rfp with 10 μM IPTG improves pinene tolerance. (c) Overexpression of Maqu_3494 (strain A-Maqu_3494/S-rfp) by IPTG induction inhibits growth. For (a-c) error bars are the standard error of three biological replicates. (d) Simulation results showing the cost and benefit of Maqu_3494 expression in an environment containing 0.5% pinene. At low induction, biofuel toxicity is substantial, while at high induction pump toxicity dominates. The total toxicity is minimized at an intermediate level. Biofuel and pump toxicities are normalized by their maximum values. (e) Experimental data showing biomass after 12 hours of growth with 0.5% pinene for the strain A-Maqu_3494/S-rfp as a function of IPTG concentration. For (a-c, e) error bars are the standard error of three biological replicates.

data from A-Maqu_3494/S-*rfp* to fit a mathematical model describing cell growth, biofuel, and pump toxicity (Methods). The model is based on the Monod growth equation (17), with modifications to account for biofuel and pump toxicity. We ran simulations for a range of inducer concentrations at a fixed pinene concentration and recorded the intracellular pinene and the final pump concentrations (Fig. 2.1d). The combined impact of biofuel and pump toxicity shows a clear minimum near 10μM IPTG, suggesting that an intermediate induction level will maximize cell growth. We validated this experimentally by growing cells in the presence of 1% pinene with varying levels of IPTG induction (Fig. 2.1e). As predicted by the model, growth in the presence of pinene is maximized at an intermediate induction level. These data highlight the trade-off between biofuel and pump toxicity for a strain with heterologous expression of a single efflux pump.

Next, we comprehensively characterized biofuel and pump toxicity for four efflux pumps. We chose three pinene and four IPTG concentrations ranging from zero to complete inhibition and induction respectively, for a total of twelve biofuel-inducer pairs. We performed growth assays using four single-pump strains: A-Pp_3456/S-*rfp*, A-Maqu_3494/S-*rfp*, A-*rfp*/S-Maqu_0582, and A-*rfp*/S-Abo_0964. In all cases, efflux pump expression is under control of the lacUV5 promoter and induced by IPTG. Recall that 0.5% pinene completely inhibits growth in the wildtype strain. Thus, the experiments with Pp_3456 and Maqu_3494 show improvements in pinene tolerance at low and moderate levels of induction (Fig. 2.2a-b). In addition, the effect of pump toxicity is visible in these strains, with higher levels of IPTG corresponding to a reduced growth rate. In contrast, the Maqu_0582 and Abo_0964 data show weak improvements in pinene tolerance and, although the pumps are toxic, as evidenced by a reduced growth rate in the absence of pinene and IPTG, further induction does not have a dramatic effect on growth (Fig. 2.2c-d). We selected these strains initially based on their improvement of pinene tolerance in a previous study (6), however differences between the strains and plasmids likely account for the reduced pump performance here. Overall, these experiments map the fitness landscapes for four individual efflux pumps under different biofuel and induction conditions, revealing trade-offs in pump expression and tolerance.

Given our data set on growth rates for biofuel and inducer pairs, we next asked whether our mathematical model could capture the fitness landscape to help predict and interpret trade-offs in pump expression. Using the experimental data, we first modeled the impact of pinene toxicity (Methods and Supplementary Information). The parameters were determined using data from the wildtype strain, A-*rfp*/S-*rfp*, and were then held constant across all subsequent simulations. Next, we used the data from each individual pump to fit the parameters associated with pump toxicity and biofuel export. The modeled fitness landscapes capture the features observed in the experimental data, including the interplay between

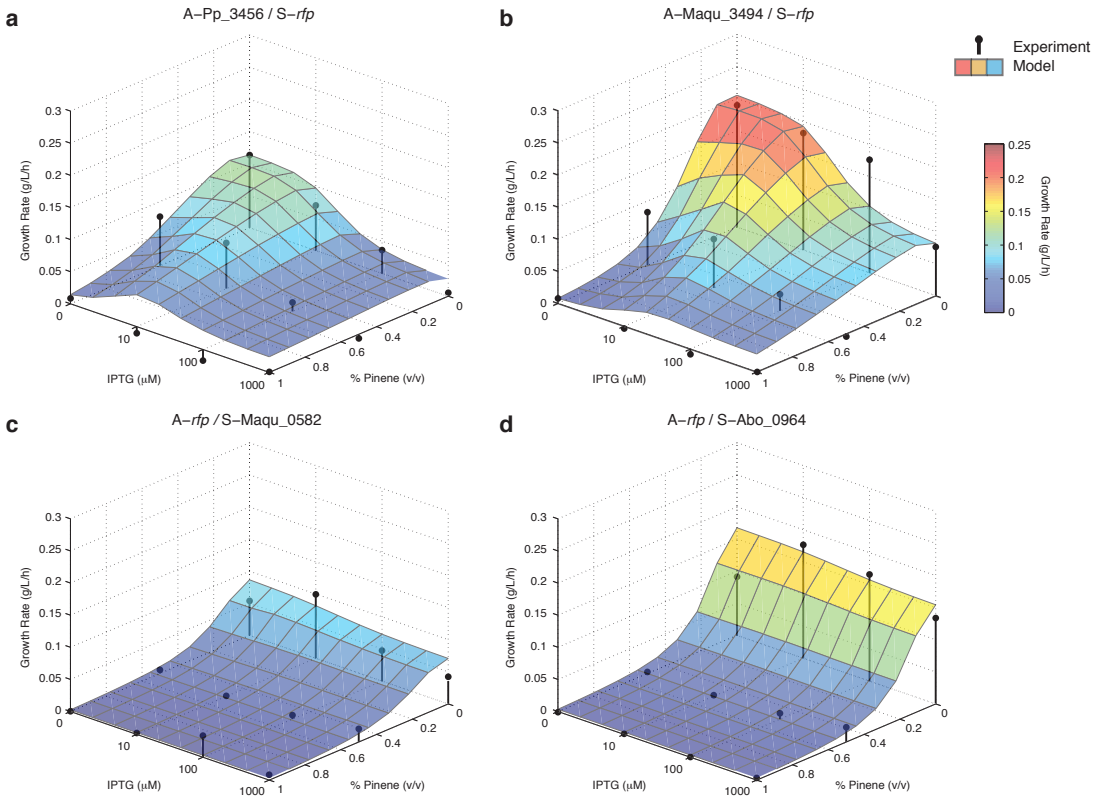

Figure 2.2: Fitness landscapes resulting from heterologous expression of single efflux pumps for a range of pinene and IPTG concentrations. Black dots represent the experimentally measured mean growth rate in exponential phase at each set of conditions. The colored surfaces show the same metric from simulated growth curves, as predicted by the mathematical model. Fitness landscapes are shown for four single-pump strains: (a) A-Pp_3456/S-rfp, (b) A-Maqu_3494/S-rfp, (c) A-rfp/S-Maqu_0582, and (d) A-rfp/S-Abo_0964. Error bars for the experimental data are shown in Fig. 2.5a and error metrics are listed in Table 2.1.

biofuel and pump toxicities for the four distinct pumps (Fig. 2.2a-d). Our modeling results are significant because they indicate that it may be possible to measure only a subset of data points in a fitness landscape, rather than exhaustively mapping all combinations. In addition, the model of individual pumps can be used to produce testable predictions about what happens when pumps are used in combination.

Using the pumps we characterized individually, we next constructed strains harboring two heterlogously expressed efflux pumps. We tested A-Pp_3456/S-Maqu_0582 and

A-Maqu_3494/S-Abo_0964 with different combinations of pinene and IPTG (Fig. 2.3a-b). Although Maqu_0582 acting alone showed little increase in pinene tolerance, the strain with both Pp_3456 and Maqu_0582 exhibited an increase in growth rate in the presence of pinene. This effect is especially noticeable at the 1% pinene concentration, where the combination of pumps outperforms the single pump strains. These results suggest that combinations of pumps, even including those that show limited benefit when expressed individually, may be able to improve tolerance. In principle, pumps from different sources could work together as chimeras using, for example, inner membrane and periplasmic proteins from one pump and outer membrane proteins from another. Previous studies have shown examples of efflux pumps that can function in this modular fashion (6, 8).

Using the model with parameters determined from the single pump strain, we were able to accurately predict the shape of the fitness landscape for both combinations of pumps (Fig. 2.3a-b). To achieve this, we used the growth rate for the strain with no pinene or IPTG to set the relative position of the fitness landscape, but otherwise changed no parameters (Methods). In other words, the parameters determined using the single pump strains, in combination with measurements from a single condition of the double pump strains, were sufficient to accurately predict the entire fitness landscape for many different biofuel and pinene combinations.

In addition to the growth rate predictions, the model can also generate predictions of growth curve data. Here, we present data for the no pump, one pump, and two pump conditions for Pp_3456 and Maqu_0582, showing that, in all cases, the model is able to accurately represent the experimental data. Again, the modeling predictions from the two pump system are based on single pump measurements. Such a model guided approach has the potential to drastically reduce the number of experimental measurements necessary to optimize biofuel tolerance.

After our success at capturing the effects of dual heterologous pump expression, we asked

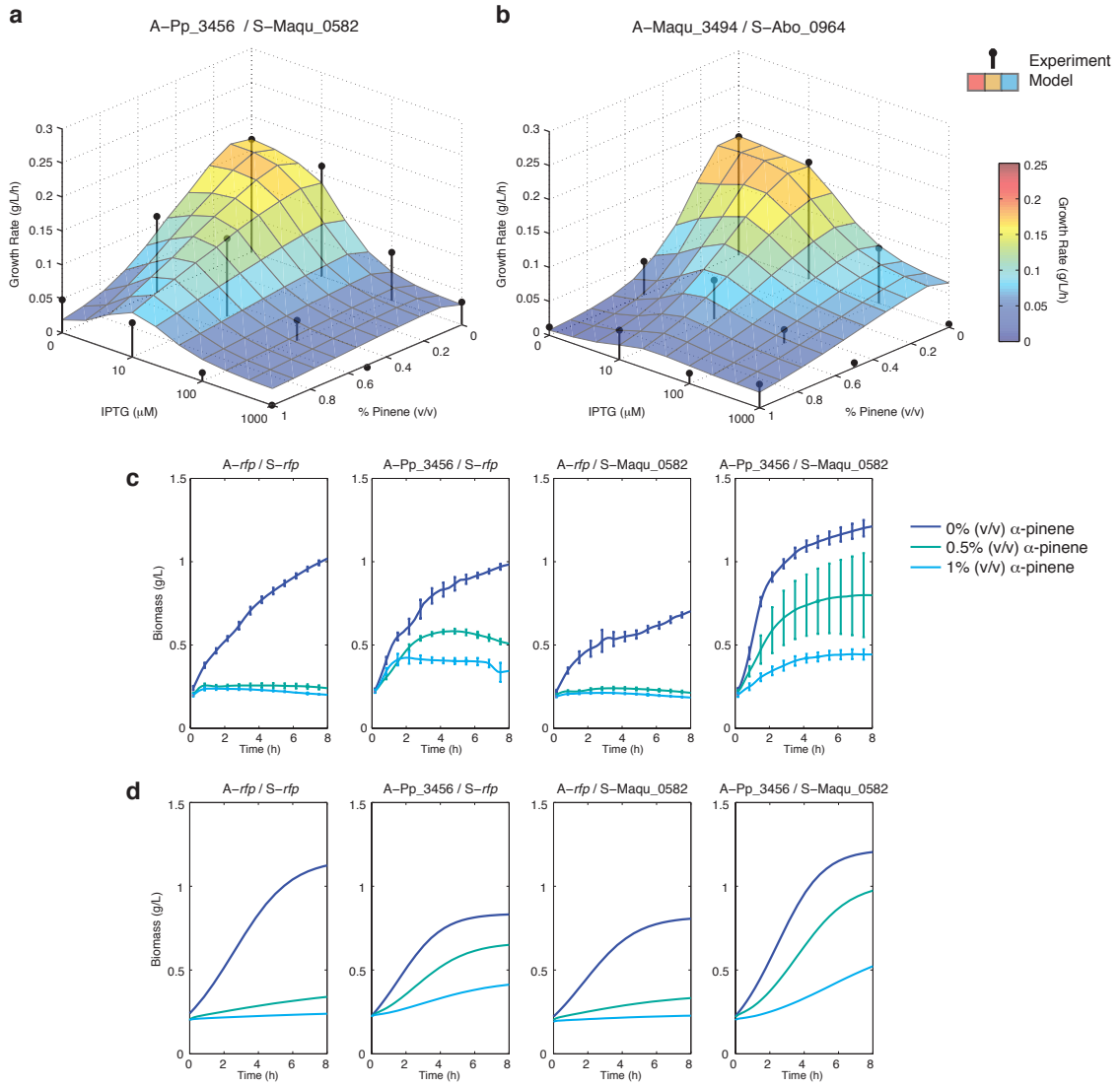

Figure 2.3: Fitness landscapes and growth curves resulting from simultaneous heterologous expression of two efflux pumps. Growth rate in exponential phase as a function of pinene and IPTG for strains with two pumps: (a) A-Pp_3456/S-Maqu_0582 and (b) A-Maqu_3494/S-Abo_0964. Black dots show experimental data; colored surface map is the modeling prediction. For error bars and analysis see Fig. 2.5b, Table 2.1. (c) Experimental growth curves for no pump, single pump, and double pump strains with 0 μm IPTG. Error bars show standard error for three replicates. (d) Mathematical modeling predictions for the same conditions as in (c).

whether the model could be used as a tool to predict the fitness landscape of a novel pump combination. To test this, we constructed A-Maqu_0582/S-Pp_3456 and A-Abo_0964/S-

Maqu_3494. We measured the baseline growth under 0% pinene and 0 μM IPTG and then switched the pump expression rates to account for the plasmid copy number swap, leaving all other aspects of the model and its parameters unchanged. We then performed growth assays with a subset of the pinene and IPTG conditions. The model shows good agreement with the experimental data (Fig. 2.4a-b), further confirming our ability to predict combinatorial pump effects. Notably, both the model and the experimental data show the superior pinene tolerance of the A-Maqu_0582/S-Pp_3456 strain (Fig. 2.4a) over the A-Abo_0964/S-Maqu_3494 strain (Fig. 2.4b). This is visible in the experimental data at 0.5% pinene, where 10 μM IPTG induction of the pumps leads to improved growth over the A-Abo_0964/S-Maqu_3494 strain. This is a non-trivial prediction, as the combined effects of the pumps without any pinene or IPTG would have suggested that this strain was inferior. We also tested A-Pp_3456/S-Maqu_3494. Individually, both pumps produced increases in pinene tolerance (Fig. 2.2a-b). When combined, pump toxicity is substantial, though the strain retains improved pinene tolerance relative to the A-rfp/S-rfp control (Fig. 2.4c).

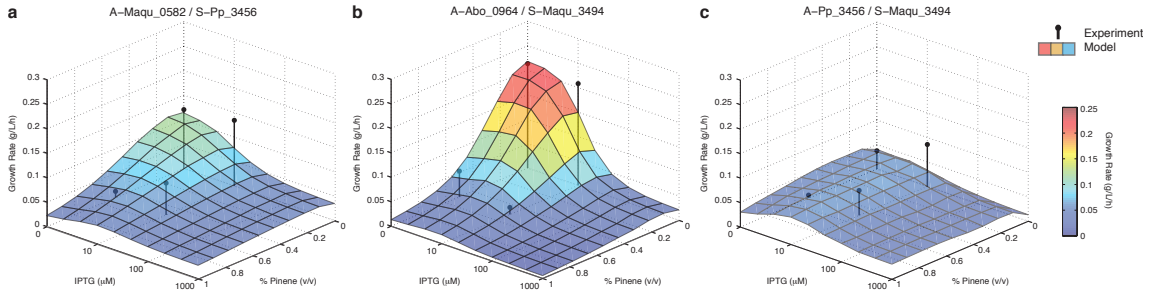

Figure 2.4: Experimental data and model predictions of fitness landscapes for pump combinations with swapped plasmid backbones. (a) A-Maqu_0582/S-Pp_3456, (b) A-Abo_0964/S-Maqu_3494 and (c) A-Pp_3456/S-Maqu_3494. Black dots show experimental data for a subset of the pinene and IPTG conditions. The surface shows modeling predictions. Note that although the baseline growth rate for the A-Abo_0964/S-Maqu_3494 combination is higher, A-Maqu_0582/S-Pp_3456 and A-Pp_3456/S-Maqu_3494 both achieve a higher growth rate at 0.5% pinene, 10 μM IPTG. The model predicts this trend to extend to higher biofuel and inducer concentrations. For error bars and analysis see Fig. 2.5c, Table 2.1.

This work provides a method for selecting efflux pumps for use in combination to improve biofuel tolerance of a host organism. By first testing single pump performance, selecting

pumps that work well with the native biofuel tolerance machinery, and then using the model to predict the performance of their combinations, it is possible to greatly reduce the number of experiments required to optimize the biofuel tolerance of a strain. Our model assumes that pump toxicity is multiplicative, which is a good approximation for the cases we tested, however even in cases where this is not valid, the model can suggest a subset of experiments to perform. A limitation of our approach is that it is necessary to measure the performance of the strain at one condition (without pinene or IPTG) in order to set the baseline growth rate. We found that some pump combinations were highly toxic even with only basal pump expression (Fig. 2.4c). In the future, improved models that capture synergistic or antagonistic effects in the absence of biofuel would be useful. For example, further experiments characterizing how heterologous pumps interact, and also potential interactions with native E. coli efflux pumps like AcrAB-TolC could further improve the model.

Optimization of pumps and their expression systems may further improve biofuel tolerance. For simplicity, we used a single inducer for both pumps, but in principle the pumps can be controlled independently. Further optimization using distinct inducible promoters is likely to better match the best induction levels for each pump. Although we used inducible promoters for this work, several recent studies have demonstrated that biosensor-based feedback can optimize growth by minimizing toxicity (3, 33). This approach can be combined with preliminary screens based on the methods presented here. In addition, the pumps used here have not been optimized for expression in E. coli; codon optimization, directed evolution, or other strategies could serve to further improve tolerance (9). The ability to accurately predict how combinations of tolerance mechanisms work together based on a small subset of experimental measurements has the potential to dramatically reduce the effort associated with engineering biofuel tolerance, leading to improved biofuel production strains.

2.3 Methods

2.3.1 Bacterial Growth Conditions

Cultures were grown in Luria Broth (LB) medium supplemented with 30 μg/ml kanamycin and 35 μg/ml chloramphenicol at 37C with 200 rpm orbital shaking. Overnight cultures were inoculated from a single colony. Pre-cultures were prepared by diluting overnight cultures 1:100 in selective LB medium and were grown for two hours. Pre-cultures were then diluted back to an optical density of approximately 0.2, IPTG was added to achieve concentrations of 0, 10, 100, or 1000 μM, and the cultures were transferred to a 48-well plate (total volume per well of 500 μl). α-pinene (Sigma) was added directly to the wells at concentrations of 0, 0.5, or 1% v/v. We note that pinene is insoluble in the growth medium and remains in a thin layer on the surface of the well. Plates were sealed with membranes to limit evaporation (Thermo Scientific AB-0580). Optical density readings and *rfp* fluorescence measurements (Supplementary Information) were taken at ten minute intervals in a BioTek Synergy H1 hybrid plate reader. All experiments were performed in triplicate.

2.3.2 Plasmids and Strains

We used plasmid vectors pBbA5k and pBbS5c from the BglBrick library (15). The *rfp* plasmids from this library were used as controls. Efflux pumps were obtained from the library developed in (15). The pumps used here include all genes on the operon, which includes the inner membrane protein and periplasmic linker for Pp_3456 and Maqu_3494, and the inner membrane, periplasmic, and outer membrane proteins for Maqu_0582 and Abo_0964. The NCBI accession number for the inner membrane protein from Pp_3456 is NP_745594, Maqu_3494 is YP_960752, Maqu_0582 is YP_957870, and Abo_0964 is YP_692684. In the

original library, the efflux pumps are on the pBbA5k vector. To make pBbS5c variants, we amplified the efflux pump genes using PCR and cloned them into the pBbS5c vector, replacing *rfp* with the coding sequences associated with all pump components, as listed in (15). Plasmids were constructed using the Gibson assembly method (11). pBbA5k and pBbS5c plasmids were co-transformed into *E. coli* BW25113 and isolated on LB plates with kanamycin (30 μg/ml) and chloramphenicol (35 μg/ml). For experiments, plasmids were freshly co-transformed and then used for replicate experiments.

2.3.3 Growth Rate and Toxicity Calculations

Optical density data at 600nm from the plate reader experiments was converted to biomass (g/L) using an approximation of 1 g/L = 0.95 OD for exponential phase *E. coli* (18). In order to eliminate single spurious data points to allow for derivative calculations, growth curves were preprocessed using a moving average filter with a window of five data points. In each window, the maximum and minimum of the subset were eliminated and the mean value of the remaining three points was calculated. Growth curve derivatives were calculated from the filtered data by taking the difference between the data points adjacent to each point and dividing by the two time intervals between them. The mean of the growth rate data in exponential phase, which we defined as 1-4 hours, was used as the metric to assess the growth rate of the culture at each set of IPTG and pinene concentrations for both the experimental and simulated data (the sensitivity of the results to the selection of this time window is given in Table 2.2. Biofuel toxicity and pump toxicity (Fig. 2.1d) were quantified as the intracellular biofuel or pump protein concentration after 100 hours of simulation time. These values were normalized by the biofuel or pump protein concentration corresponding to complete inhibition.

2.3.4 Mathematical Model

A system of ordinary differential equations was used to model the rate of change of biomass N, growth substrate S, efflux pump on the medium copy plasmid P_1 and low copy plasmid P_2, and intracellular pinene concentration C_i. Cell growth (Eqn. 2.1) and substrate consumption (Eqn. 2.2) were modeled using a modified form of the Monod equation (17), as in (10).

$$\dot{N} = \mu_{max} N \frac{S}{K_s + S} \frac{1}{1 + (\frac{C_i}{K_c})^h} \frac{1}{1 + (\frac{P_1}{K_{p1}})^{h_{p1}}} \frac{1}{1 + (\frac{P_2}{K_{p2}})^{h_{p2}}} \tag{2.1}$$

$$\dot{S} = -\frac{1}{\gamma} \mu_{max} N \frac{S}{K_s + S} \tag{2.2}$$

For single pump strains, the maximum growth rate μ_{max}, growth yield γ, and half-saturation constant K_s, were adjusted to fit the toxicity profile specific to that pump (Supplementary Information). For new pump combinations, these baseline growth parameters were set based on the growth observed in the absence of both pinene and IPTG. The half-inhibition constant for pinene K_c, and the Hill coefficient h, were fit to the data for mean exponential growth rate as a function of pinene concentration for the wildtype strain (A-*rfp*/S-*rfp* from Fig. 2.1a) (Fig. 2.6. The half-maximum inhibition constants for efflux pumps, K_{p1} and K_{p2}, and the corresponding Hill coefficients, h_{p1} and h_{p2}, were set to match the mean exponential growth rates of strains expressing the appropriate pump at the selected IPTG induction levels (Fig. 2.7). For pump combinations, we set the baseline growth parameters μ_{max}, γ, and K_s based on the growth observed in the absence of both pinene and IPTG; all other parameters are the same as those determined from the single pump experiments. Further details on model parameters and their selection is available in Supplementary Information.

Pump expression (Eqn. 2.3-2.4) was modeled using the formula for chemically inducible expression from (5), with a maximum expression rate of $\alpha_{p1/2}$ and threshold γ_I. These expression constants, along with basal expression rates $\alpha_{p01/2}$ were attained from normalized *rfp* expression data for each of the plasmids (Fig. 2.9). β is the pump protein degradation rate.

$$\dot{P_1} = \alpha_{p01} + \alpha_{p1}\frac{I}{I+\gamma_I} - \beta P_1 \tag{2.3}$$

$$\dot{P_2} = \alpha_{p02} + \alpha_{p2}\frac{I}{I+\gamma_I} - \beta P_2 \tag{2.4}$$

To model intracellular pinene concentration, a biofuel mass balance was incorporated to ensure that while mass could pass between the intracellular and extracellular domains, the total mass of pinene in the entire domain was constant. Passive diffusion of pinene through the cell membrane and export by efflux pumps was modeled by Eqn. 2.5, as in (10), where C_i and C_e are the intra and extracellular pinene concentrations.

$$\dot{C_i} = \alpha_{c0}\frac{V_e}{V_i}(C_e - C_i) - C_i(\alpha_{c1}P_1 + \alpha_{c2}P_2) \tag{2.5}$$

The gradient of biofuel concentration across the cell membrane drives diffusion (4), and the concentration change is accounted for by the ratio between the intracellular and extracellular volumes (V_i and V_e) and the membrane permeability constant α_{c0}. The rate of export of biofuel due to efflux pumps depends on the intracellular pinene concentration, the pump protein concentration, and the rate of export of each pump $\alpha_{c1/2}$, which were set to match experimental data for each individual pump. All model constants are listed in Supplementary Information (Tables 2.3 and 2.4).

Eq. 2.1 uses the pump concentrations to improve growth through a reduction in toxicity. Note that higher pump levels do not necessarily correspond to improved growth. For instance, a pump might be toxic, but not provide tolerance improvements.

All simulations were performed in MATLAB (MathWorks) using the ode23s solver.

Bibliography

[1] Atsumi, S., Hanai, T. and Liao, J. C. Non-fermentative pathways for synthesis of branched-chain higher alcohols as biofuels. Nature 451, 86 to 89. (2008).

[2] Brennan, T. C. R., Turner, C. D., Krömer, J. O., and Nielsen, L. K. Alleviating monoterpene toxicity using a two-phase extractive fermentation for the bioproduction of jet fuel mixtures in Saccharomyces cerevisiae. Biotechnology and Bioengineering, 109(10), 2513 to 22. (2012).

[3] Dahl, M. K., Msadek, T., Kunst, F., and Rapoport, G. The phosphorylation state of the DegU response regulator acts as a molecular switch allowing either degradative enzyme synthesis or expression of genetic competence in Bacillus subtilis. Journal of Biological Chemistry, 267(20), 14509-14514. (1992).

[4] Deris, J. B., Kim, M., Zhang, Z., Okano, H., Hermsen, R., Groisman, A., and Hwa, T. The innate growth bistability and fitness landscapes of antibiotic-resistant bacteria. Science (New York, N.Y.), 342(6162). (2013).

[5] Dunlop, Mary J., Jay D. Keasling, and Aindrila Mukhopadhyay. A model for improving microbial biofuel production using a synthetic feedback loop. Systems and synthetic biology 4.2, 95-104. (2010).

[6] Dunlop, Mary J., Zain Y. Dossani, Heather L. Szmidt, Hou Cheng Chu, Taek Soon Lee, Jay D. Keasling, Masood Z. Hadi, and Aindrila Mukhopadhyay. Engineering microbial biofuel tolerance and export using efflux pumps. Molecular systems biology 7, no. 1 (2011).

[7] Dunlop, Mary J. Engineering microbes for tolerance to next-generation biofuels. Biotechnol Biofuels 4.1: 32. (2011).

[8] Elkins, C.A. and H. Nikaido. Substrate specificity of the RND-type multidrug efflux pumps AcrB and AcrD of Escherichia coli is determined predominately by two large periplasmic loops. Journal Of Bacteriology, 184(23): p. 6490-6498. (2002).

[9] Fisher, M. A., Boyarskiy, S., Yamada, M. R., Kong, N., Bauer, S., and Tullman-Ercek, D.. Enhancing tolerance to short-chain alcohols by engineering the *Escherichia coli* AcrB efflux pump to secrete the non-native substrate n-butanol. ACS synthetic biology, 3(1), 30-40. (2013).

[10] Frederix, M., K. Hutter, J. Leu, T. S. Bath, W. J. Turner, T. L. Rüegg, H. W. Blanch, B. D. Simmons, P. D. Adams, J. D. Keasling, M. P. Thelen, M. J. Dunlop, C. J. Petzold, A. Mukhopadhyay. Development of a Native *Escherichia coli* Induction System for Ionic Liquid Tolerance. PloS one, 9(7), e101115. (2014).

[11] Gibson, D. G., Young, L., Chuang, R. Y., Venter, J. C., Hutchison, C. A., and Smith, H. O.. Enzymatic assembly of DNA molecules up to several hundred kilobases. Nature methods, 6(5), 343-345. (2009).

[12] Harrison, M. E., and Dunlop, M. J.. Synthetic feedback loop model for increasing microbial biofuel production using a biosensor. Frontiers in microbiology, 3. (2012).

[13] Harvey, Benjamin G., Michael E. Wright, and Roxanne L. Quintana. High-density renewable fuels based on the selective dimerization of pinenes. Energy and Fuels 24.1, 267-273. (2009).

[14] Huu, N. B., Denner, E. B., Ha, D. T., Wanner, G., and Stan-Lotter, H.. Marinobacter aquaeolei sp. nov., a halophilic bacterium isolated from a Vietnamese oil-producing well. International journal of systematic bacteriology, 49(2), 367-375. (1999).

[15] Lee, Taek Soon, Rachel A. Krupa, Fuzhong Zhang, Meghdad Hajimorad, William J. Holtz, Nilu Prasad, Sung Kuk Lee, and Jay D. Keasling. BglBrick vectors and datasheets: a synthetic biology platform for gene expression. Journal of biological engineering 5, no. 1: 1-14. (2011).

[16] Lee, Angela, Weimin Mao, Mark S. Warren, Anita Mistry, Kazuki Hoshino, Ryo Okumura, Hiroko Ishida, and Olga Lomovskaya. Interplay between efflux pumps may provide either additive or multiplicative effects on drug resistance. Journal of bacteriology 182, no. 11, 3142-3150. (2000).

[17] Jacques Monod. The growth of bacterial cultures. Annual Reviews in Microbiology. (1949).

[18] Neidhardt, F., Escherichia coli and Salmonella: cellular and molecular biology. (1996).

[19] Nelson, K. E., Weinel, C., Paulsen, I. T., Dodson, R. J., Hilbert, H., Martins dos Santos, V. A. P., Fouts, D. E., Gill, S. R., Pop, M., Holmes, M., Brinkac, L., Beanan, M., DeBoy, R. T., Daugherty, S., Kolonay, J., Madupu, R., Nelson, W., White, O., Peterson, J., Khouri, H., Hance, I., Lee, P. C., Holtzapple, E., Scanlan, D., Tran, K., Moazzez, A., Utterback, T., Rizzo, M., Lee, K., Kosack, D., Moestl, D., Wedler, H., Lauber, J., Stjepandic, D., Hoheisel, J., Straetz, M., Heim, S., Kiewitz, C., Eisen, J., Timmis, K. N., Düsterhöft, A., Tümmler, B. and Fraser, C. M.. Complete genome sequence and comparative analysis of the metabolically versatile Pseudomonas putida KT2440. Environmental Microbiology, 4: 799-808. (2002).

[20] Nicolaou, S. a, Gaida, S. M., and Papoutsakis, E. T.. A comparative view of metabolite and substrate stress and tolerance in microbial bioprocessing: From biofuels and chemicals, to biocatalysis and bioremediation. Metabolic Engineering, 12(4), 307 to 31. (2010).

[21] Peralta-Yahya, Pamela P., Fuzhong Zhang, Stephen B. Del Cardayre, and Jay D. Keasling. Microbial engineering for the production of advanced biofuels. Nature 488, no. 7411, 320-328. (2012).

[22] Ramos, Juan L., Estrella Duque, MaríaTrinidad Gallegos, Patricia Godoy, María Isabel Ramos-González, Antonia Rojas, Wilson Terán, and Ana Segura. Mechanisms of solvent tolerance in gram-negative bacteria. Annual Reviews in Microbiology 56, no. 1, 743 to 768. (2002).

[23] Rojas, Antonia, Estrella Duque, Gilberto Mosqueda, Geir Golden, Ana Hurtado, Juan L. Ramos, and Ana Segura. Three Efflux Pumps Are Required To Provide Efficient Tolerance to Toluene in Pseudomonas putida DOT-T1E. Journal of bacteriology 183, no. 13: 3967-3973. (2001).

[24] Sarria, S., Wong, B., Martín, H. G., Keasling, J. D., and Peralta-Yahya, P.. Microbial Synthesis of Pinene. ACS Synthetic Biology. (2014).

[25] Schneiker, S., dos Santos, V. A. M., Bartels, D., Bekel, T., Brecht, M., Buhrmester, J., and Golyshin, P. N.. Genome sequence of the ubiquitous hydrocarbon-degrading marine bacterium Alcanivorax borkumensis. Nature biotechnology, 24(8), 997-1004.(2006).

[26] Segura, A., Molina, L., Fillet, S., Krell, T., Bernal, P., Muñoz-Rojas, J., and Ramos, J. L.. Solvent tolerance in Gram-negative bacteria. Current opinion in biotechnology, 23(3), 415-421. (2012).

[27] Singer, E., Webb, E. A., Nelson, W. C., Heidelberg, J. F., Ivanova, N., Pati, A., and Edwards, K. J.. Genomic potential of Marinobacter aquaeolei, a biogeochemical ŇopportunitrophÓ. Applied and environmental microbiology, 77(8), 2763-2771. (2011).

[28] Teixeira, M. C., Godinho, C. P., Cabrito, T. R., Mira, N. P., and Sá-Correia, I.. Increased expression of the yeast multidrug resistance ABC transporter Pdr18 leads to increased ethanol tolerance and ethanol production in high gravity alcoholic fermentation. Microb Cell Fact, 11(1), 1-9. (2012).

[29] Wagner, S., Baars, L., Ytterberg, a J., Klussmeier, A., Wagner, C. S., Nord, O., É de Gier, J.-W. Consequences of membrane protein overexpression in *Escherichia coli*. Molecular and Cellular Proteomics : MCP, 6(9), 1527-50. (2007).

[30] Wood, K. B., and Cluzel, P.. Trade-offs between drug toxicity and benefit in the multi-antibiotic resistance system underlie optimal growth of E . coli. (2012).

[31] Yakimov, M. M., Golyshin, P. N., Lang, S., Moore, E. R., Abraham, W. R., Lünsdorf, H., and Timmis, K. N.. Alcanivorax borkumensis gen. nov., sp. nov., a new, hydrocarbon-degrading and surfactant-producing marine bacterium. International journal of systematic bacteriology, 48(2), 339-348. (1998).

[32] Yang, Jianming, Qingjuan Nie, Meng Ren, Hongru Feng, Xinglin Jiang, Yanning Zheng, Min Liu, Haibo Zhang, and Mo Xian. "Metabolic engineering of Escherichia coli for the biosynthesis of alpha-pinene." Biotechnol Biofuels 6: 60. (2013).

[33] Zhang, F., Carothers, J. M., and Keasling, J. D.. Design of a dynamic sensor-regulator system for production of chemicals and fuels derived from fatty acids. Nature biotechnology, 30(4), 354-359. (2012).

2.4 Supplementary Information

2.4.1 Supplementary Tables

Table 2.1: Error between model and experimental data. The error is defined as the absolute value of the difference between the model and the mean of the experimental data. Statistics were taken over all experimental data points: 12 conditions for those strains shown in Figs. 2-3 and 4 conditions for Fig. 4 strains.

Strain	**Mean Error** (g/L/h)	**Maximum Error** (g/L/h)	**Sum of Squares** $(g/L/h)^2$
A-Pp_3456 / S-rfp	0.027	0.060	0.013
A-Maqu_3494 / S-rfp	0.036	0.071	0.021
A-rfp / S-Maqu_0582	0.014	0.034	0.004
A-rfp / S-Abo_0964	0.014	0.077	0.007
A-Pp_3456 / S-Maqu_0582	0.023	0.051	0.009
A-Maqu_3494 / S-Abo_0964	0.022	0.061	0.010
A-Maqu_0582 / S-Pp_3456	0.028	0.059	0.005
A-Abo_0964 / S-Maqu_3494	0.031	0.066	0.008
A-Pp_3456 / S-Maqu_3494	0.025	0.053	0.004

Table 2.2: Error as a function of the time window over which the growth rate is calculated. The error is defined as in Table 2.1. The strain data used for these calculations is from A-Pp_3456 / S-Maqu_0582.

Time Window	**Mean Error** (g/L/h)	**Maximum Error** (g/L/h)	**Sum of Squares** $(g/L/h)^2$
1-4 hours	0.023	0.051	0.009
2-5 hours	0.049	0.102	0.041
0-3 hours	0.060	0.137	0.065

Table 2.3: Model Constants

Symbol	Units	Description	Value
K_c	% v/v	Biofuel toxicity half-inhibition	0.25
h	Dimensionless	Biofuel toxicity exponent	2.0
α_{c0}	1/h	Membrane permeability constant	0.001
V_c	L	Approx. vol. of a cell (1)	1×10^{-15}
m_c	g	Mass of a cell (2)	9.5×10^{-13}
α_{p01}	protein concentration/h	med. copy basal expression rate	0.092
α_{p1}	protein concentration/h	med. copy maximum expression rate	0.79
α_{p02}	protein concentration/h	low copy basal expression rate	0.056
α_{p2}	protein concentration/h	low copy maximum expression rate	0.21
γ_I	mM IPTG	Inducer threshold	0.014
β	1/h	Pump protein degradation rate	1.0

Table 2.4: Strain and pump dependent model parameters

Symbol	Units	Description	Value
μ_{max}	1/h	Maximum growth rate	A-*rfp*, S-*rfp*: 3.0 A-Pp_3456, S-*rfp*: 3.0 A-*rfp*, S-Maqu_0582: 3.5 A-Maqu_3494, S-*rfp*: 3.0 A-*rfp*, S-Abo_0964: 3.5 A-Pp_3456, S-Maqu_0582: 2.5 A-Maqu_3494, S-Abo_0964: 2.7 A-Maqu_0582, S-PP_3456: 3 A-Abo_0964, S-Maqu_3494: 2.5 A-Pp_3456, S-Maqu_3494: 3.4
K_s	A.U.	Affinity constant	A-*rfp*, S-*rfp*: 6.0 A-Pp_3456, S-*rfp*: 3.8 A-*rfp*, S-Maqu_0582: 6.0 A-Maqu_3494, S-*rfp*: 3.0 A-*rfp*, S-Abo_0964: 4.0 A-Pp_3456, S-Maqu_0582: 2.8 A-Maqu_3494, S-Abo_0964: 3.0 A-Maqu_0582, S-Pp_3456: 5.0 A-Abo_0964, S-Maqu_3494: 3.0 A-Pp_3456, S-Maqu_3494: 3.5
γ	Dimensionless	Substrate to biomass conversion rate	A-*rfp*, S-*rfp*: 0.92 A-Pp_3456, S-*rfp*: 0.61 A-*rfp*, S-Maqu_0582: 0.6 A-Maqu_3494, S-*rfp*: 1.05 A-*rfp*, S-Abo_0964: 0.9 A-Pp_3456, S-Maqu_0582: 1.0 A-Maqu_3494, S-Abo_0964: 1.0 A-Maqu_0582, S-Pp_3456: 0.65 A-Abo_0964, S-Maqu_3494: 1.04 A-Pp_3456, S-Maqu_3494: 0.33
K_p	A.U.	Pump toxicity half-inhibition constant	Pp_3456: 0.65 Maqu_3494: 0.8 Maqu_0582: 0.6 Abo_0964: 0.5
h_p	Dimensionless	Pump toxicity exponent	Pp_3456: 4.0 Maqu_3494: 4.0 Maqu_0582: 2.0 Abo_0964: 4.0
α_c	1/h	Pump export rate	Pp_3456: 75 Maqu_3494: 30 Maqu_0582: 10 Abo_0964: 1

2.4.2 Supplementary Figures

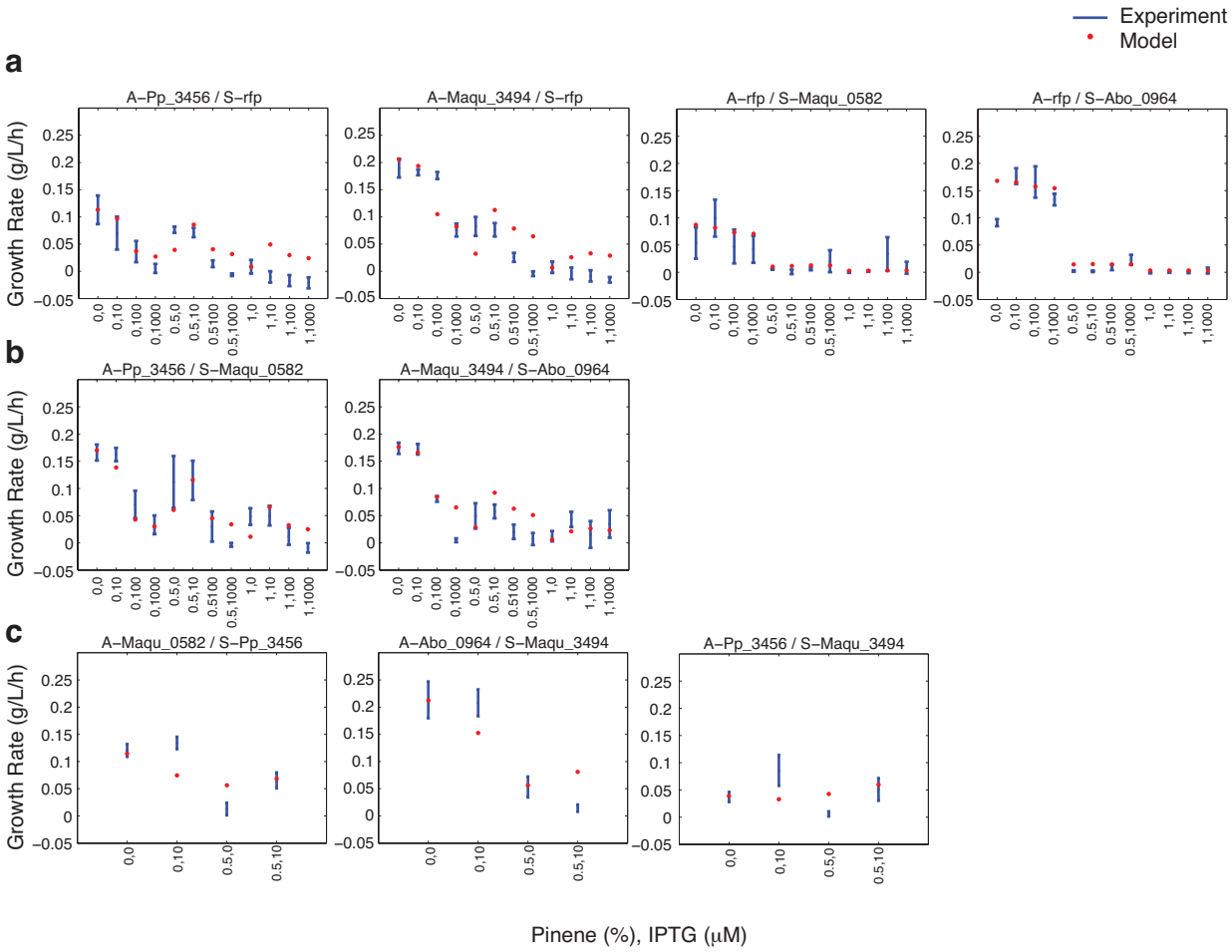

Figure 2.5: Comparison between model predictions and experimental data with error bars. The values listed on the x-axis are the pinene levels (%), followed by the IPTG levels (μM) **(a)** *corresponds with the surface plot data from Fig. 2 in the main text,* **(b)** *corresponds with Fig. 3a-b, and* **(c)** *corresponds with Fig. 4. Error bars are standard error of three biological replicates.*

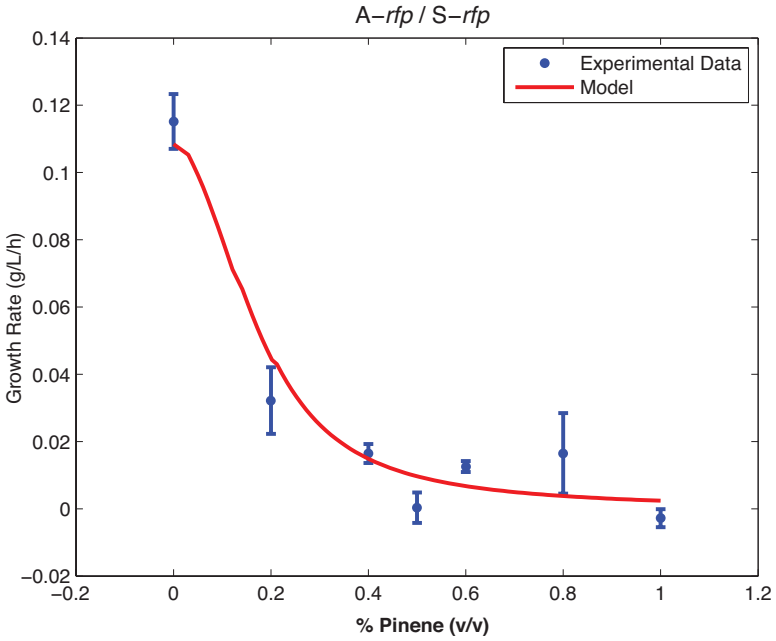

Figure 2.6: Determination of the inhibition parameters for pinene, K_c and h. The strain A-rfp/S-rfp was grown in the presence of increasing concentrations of pinene. The values of K_c and h were determined based on experimental data (blue). The model is shown in red. Error bars indicate standard error over at least two replicates for each condition.

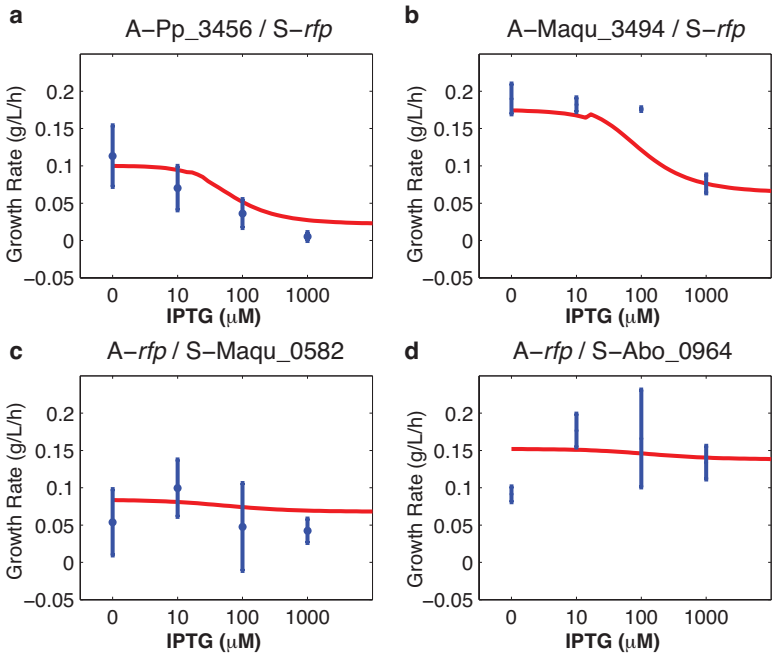

Figure 2.7: Pump toxicity profiles for E. coli strains containing single heterologous efflux pumps, **(a)** *A-Pp_3456/S-rfp,* **(b)** *A-Maqu_3494/S-rfp,* **(c)** *A-rfp/S-Maqu_0582,* **(d)** *A-rfp/S-Abo_0964. The mean growth rate during exponential phase is given as a function of IPTG concentration. The data shown here correspond to the edges of the surfaces at 0% pinene in Figure 2 of the main text. Blue data points and error bars represent mean and standard error of three biological replicates. Red lines show simulation results for the range of IPTG concentrations indicated. These data determine the model parameters K_p and h_p for each individual pump, which remain the same throughout all simulations presented in this study.*

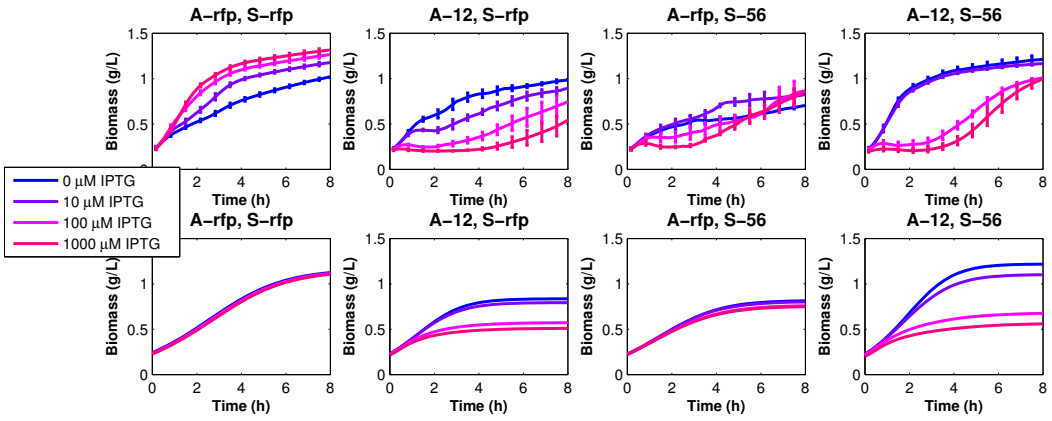

Figure 2.8: Combined toxicity of efflux pumps. Growth curves are shown from experimental data (top) and from the model (bottom) for strains containing single pumps (epl12 and epl56), the combination of the two pumps, and the negative control. Here, we can see how the pump toxicities from the individual pumps combine. The combination strain is less inhibited at lower inducer concentrations and more inhibited at higher concentrations due to the multiplication of the two pump toxicity terms, each of which has an associated Hill coefficient. Also, we consistently observed an increasing growth rate with increasing inducer concentration in the negative control (A-rfp/S-rfp). The cause of this effect is unknown and we did not attempt an explanation.

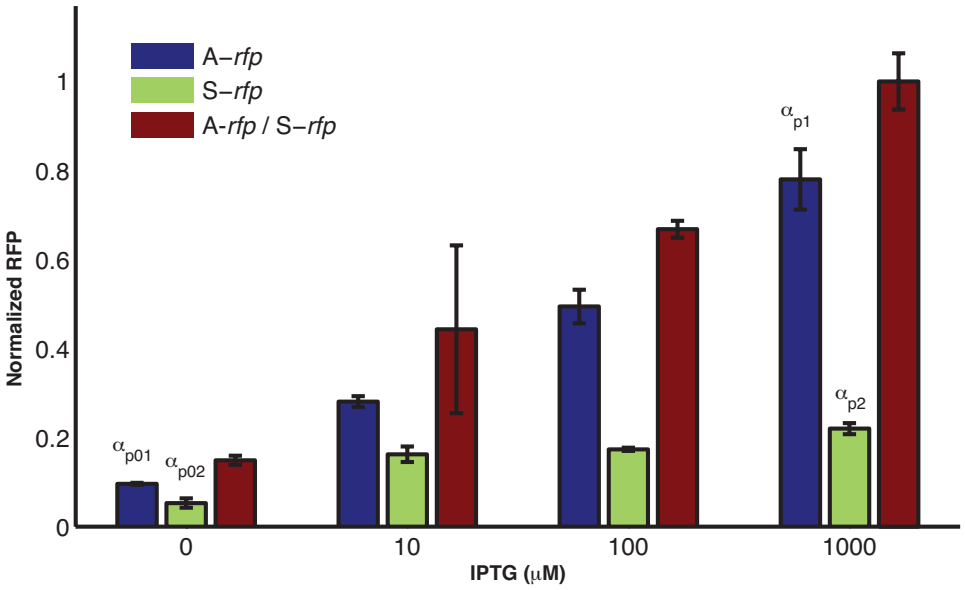

Figure 2.9: Normalized fluorescent protein data used to determine basal, $\alpha_{p01/2}$, and maximum protein expression rates, $\alpha_{p1/2}$. Values are indicated on the graph. Subscript 1 corresponds to the medium copy plasmid, pBbA5k, and subscript 2 indicates the low copy plasmid, pBbS5c. To determine $\alpha_{p01/2}$ and $\alpha_{p1/2}$, rfp was measured for each individual plasmid (A-rfp and S-rfp) and the combined plasmid strain (A-rfp/S-rfp). The ratio of the rfp measurements for single plasmid strains was used to determine the relative values of the expression rates in the two plasmid strain for each IPTG concentration. Fluorescence data were normalized by the maximum reading achieved by the strain containing both plasmids at 1000 μM IPTG. Note that the sum of the heights of the individual plasmid bars adds up to the height of the two plasmid bar since the numbers shown are rfp ratios. These data are similar to results obtained using the same plasmids, but where only one contains rfp (data not shown).

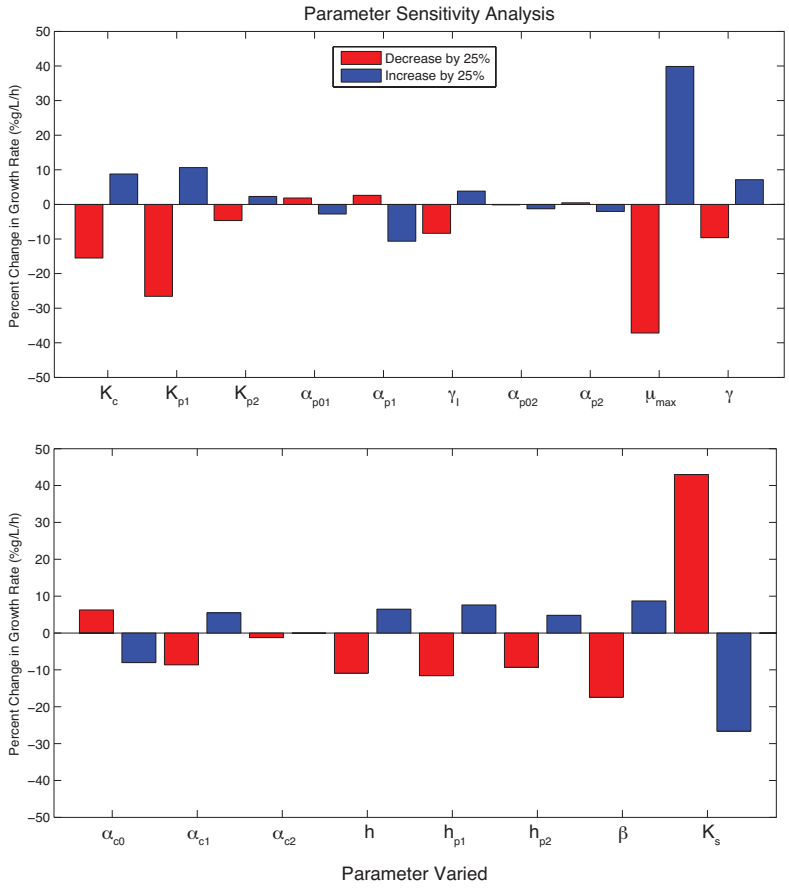

Figure 2.10: Parameter sensitivity analysis. The strain used in this analysis is the two pump strain A-Pp_3456/S-Maqu_0582 with 0.5% pinene and 10 μM IPTG. Each model parameter was first decreased (red) then increased (blue) by 25% of its original value. The height of each bar indicates the percent change in the modeled mean exponential growth rate resulting from the indicated change in each parameter.

Bibliography

[1] Phillips, R., Kondev, J., Theriot, J., and Garcia, H.. Physical biology of the cell (pp. 281-321). New York: Garland Science. (2009).

[2] Neidhardt, F.. Escherichia coli and Salmonella: Cellular and molecular biology. ASM Press. (1996).

Chapter 3

Additional Biofuel Toxicity and Efflux Pump Experiments

3.1 Background

In this chapter, we will describe additional experimental data assessing the effectiveness of several efflux pumps when used with and without AcrAB-TolC.

We have tested various efflux pump genes that were identified in a previous study (1) for an increased tolerance to α-pinene when used in combination with the native efflux pump system, AcrAB-TolC. The wild-type strain used here is *E. coli* BW25113. We obtained a knockout strain with the transporter protein AcrB deleted from the genome, this strain is referred to as *E. coli* BW25113 $\Delta acrB$ (4). This deletion has been shown previously to effectively disable the whole AcrAB-TolC system (3).

Table 3.1: Efflux pump aliases. This table lists the names used to refer to the same efflux pump. We use both naming systems interchangeably throughout this thesis.

Pump name (Chapter 2)	**Alias**
Pp_3456	epl12
Pp_3426	epl14
Maqu_3494	epl55
Maqu_0582	epl56
Abo_0964	epl95

Into these two strains (BW25113 and BW25113 Δ*acrB*), we transformed plasmids containing efflux pump genes. The efflux pump genes used here were originally identified in bacteria that demonstrated an ability to survive in toxic environments. The pumps, epl12 and epl14, are from the bacteria *Pseudomonas putida* KT2440, a derivative of *P. putida* mt-2 which was isolated from a planted field in Japan (5). The next two pumps, epl55 and epl56, are from *Marinobacter aquaeoli*, a bacteria discovered at the head of an oil producing well in Vietnam (2, 7). Lastly, epl95 comes from *Alcanivorax borkumensis* SK2, a hydrocarbon degrading bacteria discovered in the North Sea (6, 8). The two naming conventions for these pumps are described in Table 3.1, in this chapter we will use the epl naming system. We also constructed two control strains with a fluorescent protein gene in place of the efflux pump gene.

3.2 Results

All of the heterologous efflux pump genes were controlled by the IPTG inducible PlacUV5 promoter. We tested these strains for tolerance to α-pinene by growing them in a solution containing 2% v/v of α-pinene. The results of these experiments are summarized in Figure 3.1 where the final optical density of the culture for 3 replicates is plotted on a color scale. The entire growth curves are shown in Figure 3.2. Although the strain harboring epl12 does not grow to a high OD in 2% pinene, we see that in the absence of pinene the strain grows faster and to a higher OD than the wildtype strain, this is an aspect of this pump that we sought to take advantage of when used in combination with other pumps.

We found that some pump combinations seem to cooperate with AcrB (epl56) whereas other pumps that work well in the knockout strain (epl14) appear to be highly inhibitory to cell growth when expressed simultaneously with *acrB*. The efflux pumps, epl12 and epl56 were selected for further study due to their apparent cooperation with AcrB.

Next, we constructed strains containing all possible combinations of the three efflux pumps of interest, AcrB, epl12, and epl56. We tested them again by growing them in an LB solution containing either 0 or 2% α-pinene. Figure 3.3 shows the growth curves for these experiments. The results indicate an increasing tolerance to α-pinene with an increasing number of cooperative efflux pumps.

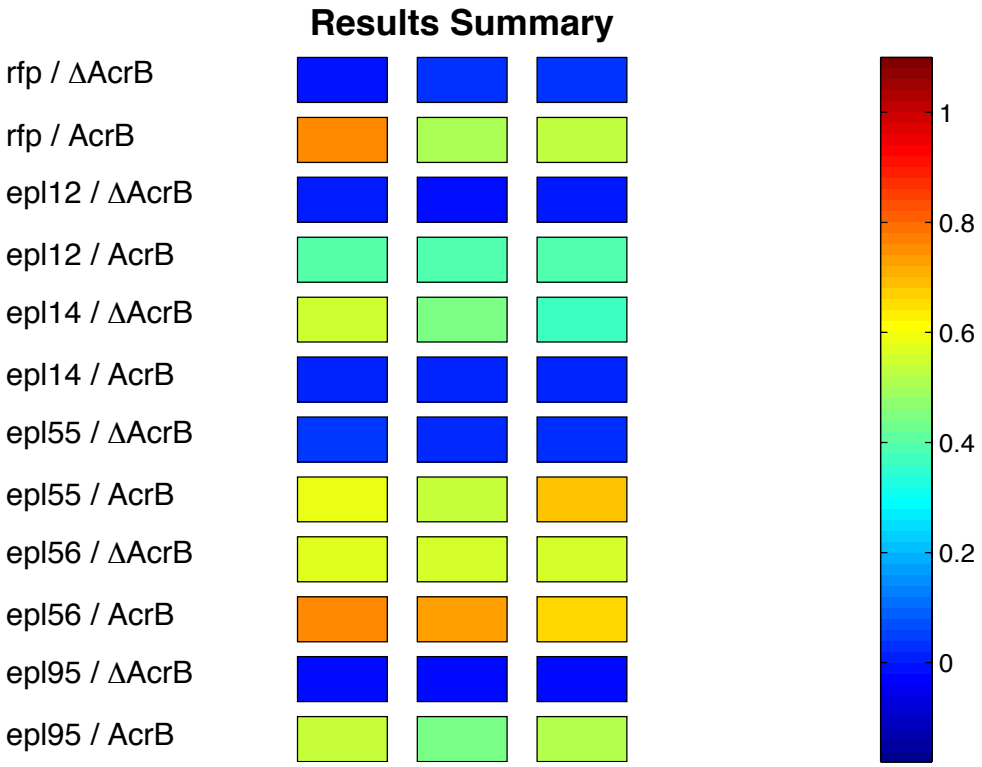

Figure 3.1: Optical density of cultures at Time=14h. Grown in LB media with 2% v/v pinene. The results from three individual replicates are shown for each strain.

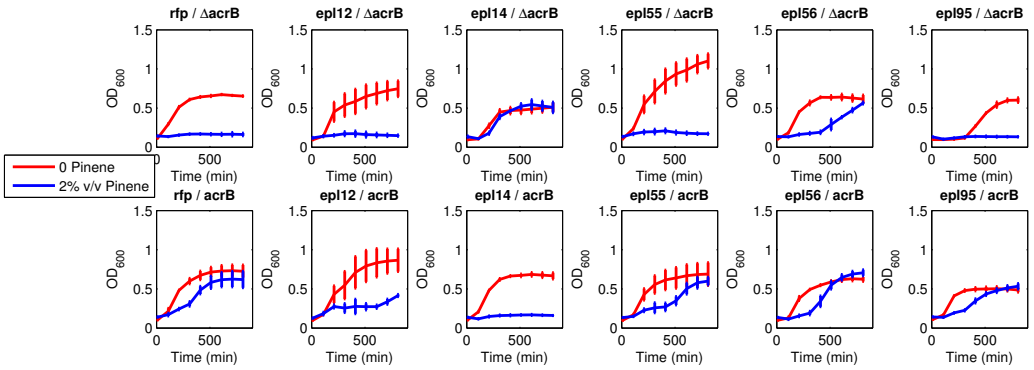

Figure 3.2: Single pump data with knockout strains. Growth curves of single pump strains with and without acrB knocked out at 0% and 2% pinene. 10 μM IPTG was used to ensure pump activity.

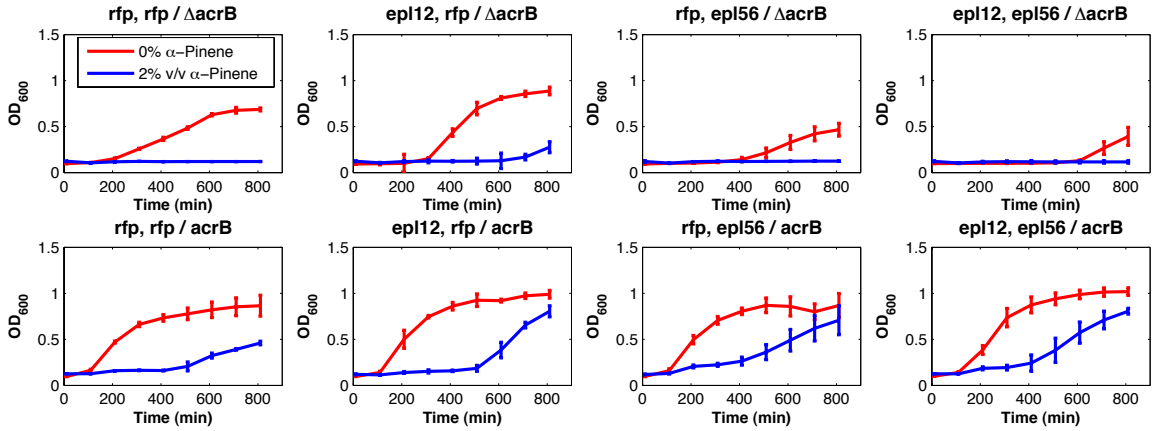

Figure 3.3: Optical density curves for E. coli strains with all possible combinations of the 3 efflux pumps of interest. Strain information is located in the title of each set of axes, 'ΔacrB' indicates the acrB knockout strain while 'acrB' represents wildtype BW25113.

In addition to the pump combinations that were presented in Chapter 2, we also tested several others using the same two plasmid platform for pump expression. We performed growth assays under four different sets of inducer/biofuel concentrations. The experiments were performed and the raw data was filtered and analyzed in the same manner described in the Methods section of Chapter 2. Figure 3.4 shows the toxicity profiles (model) for four different pump combinations along with the four experimentally measured datapoints. Figure 3.5 shows the measured and model generated growth curves for the data summarized in Figure 3.4.

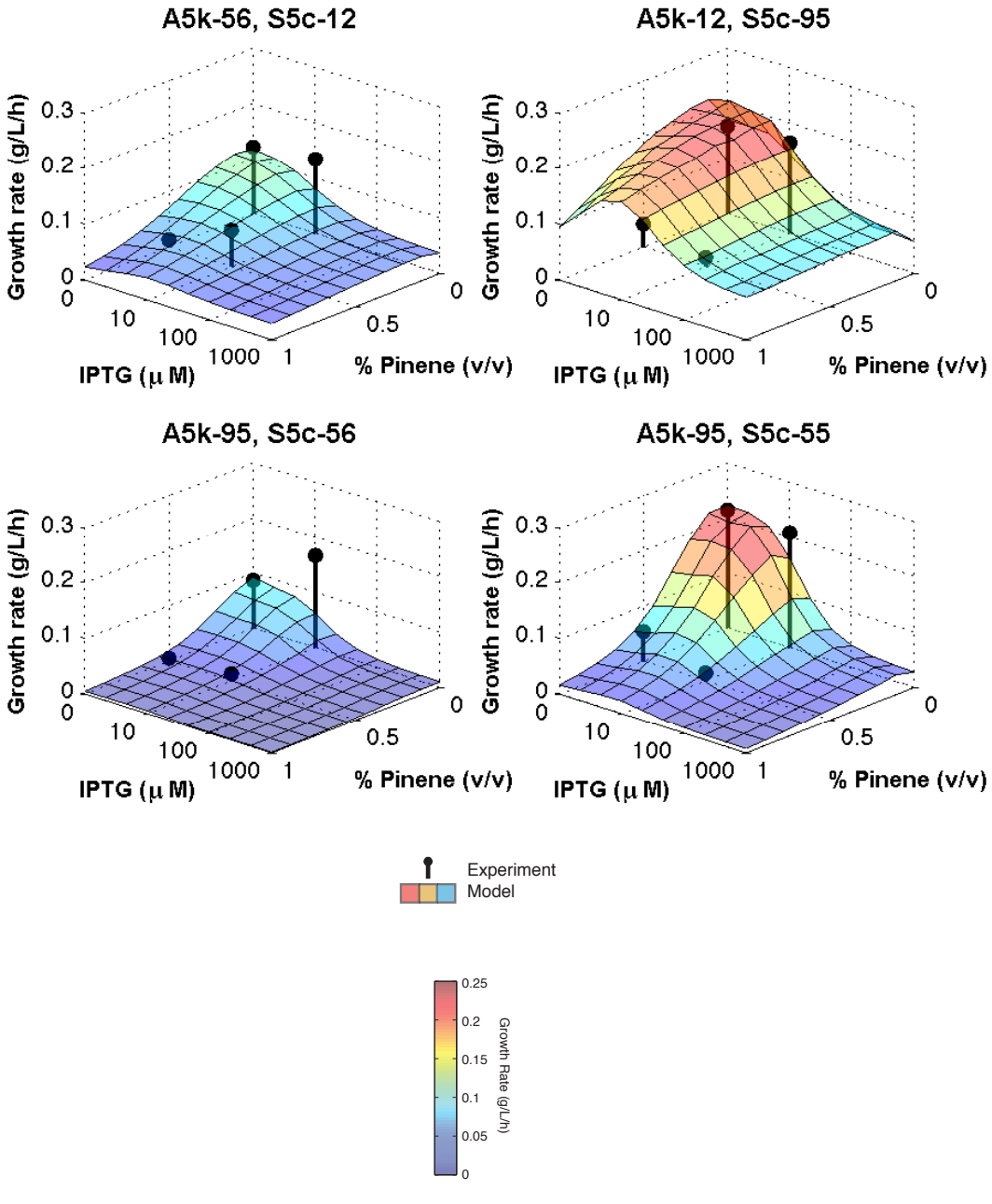

Figure 3.4: Toxicity profiles of four additional pump combinations tested. Black lines and dots represent experimentally measured growth rates and colored surfaces are modeling results.

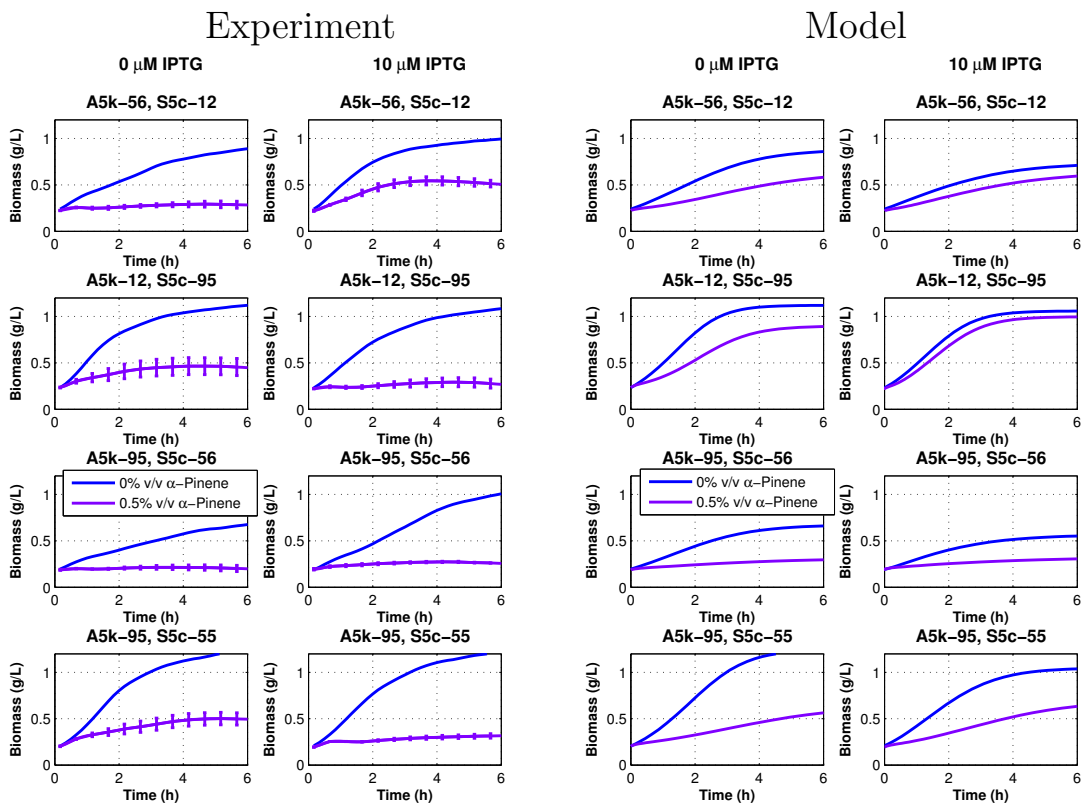

Figure 3.5: Growth curves of four additional pump combinations tested. (Left) Experimental data, error bars represent standard error for 3 biological replicates. (Right) Model generated growth curves for the same conditions. In each set of figures, the left column has 0 μM IPTG and the right column is with 10μM IPTG as indicated by the text directly above each column. The strain information is given in the titles.

Another set of four different combinations was tested as well. In this experiment we tried combining the two best individually performing pumps (epl12 and epl55), we also tried the combination of the two pumps from *M. aquaeoli* (epl55 and epl56). We constructed strains with these two pump combinations in both of the possible medium/low copy plasmid configurations for a total of four strains. The fitness landscapes for these four strains are shown in Figure 3.6 and the experimental and modeled growth curves are shown in Figure 3.7.

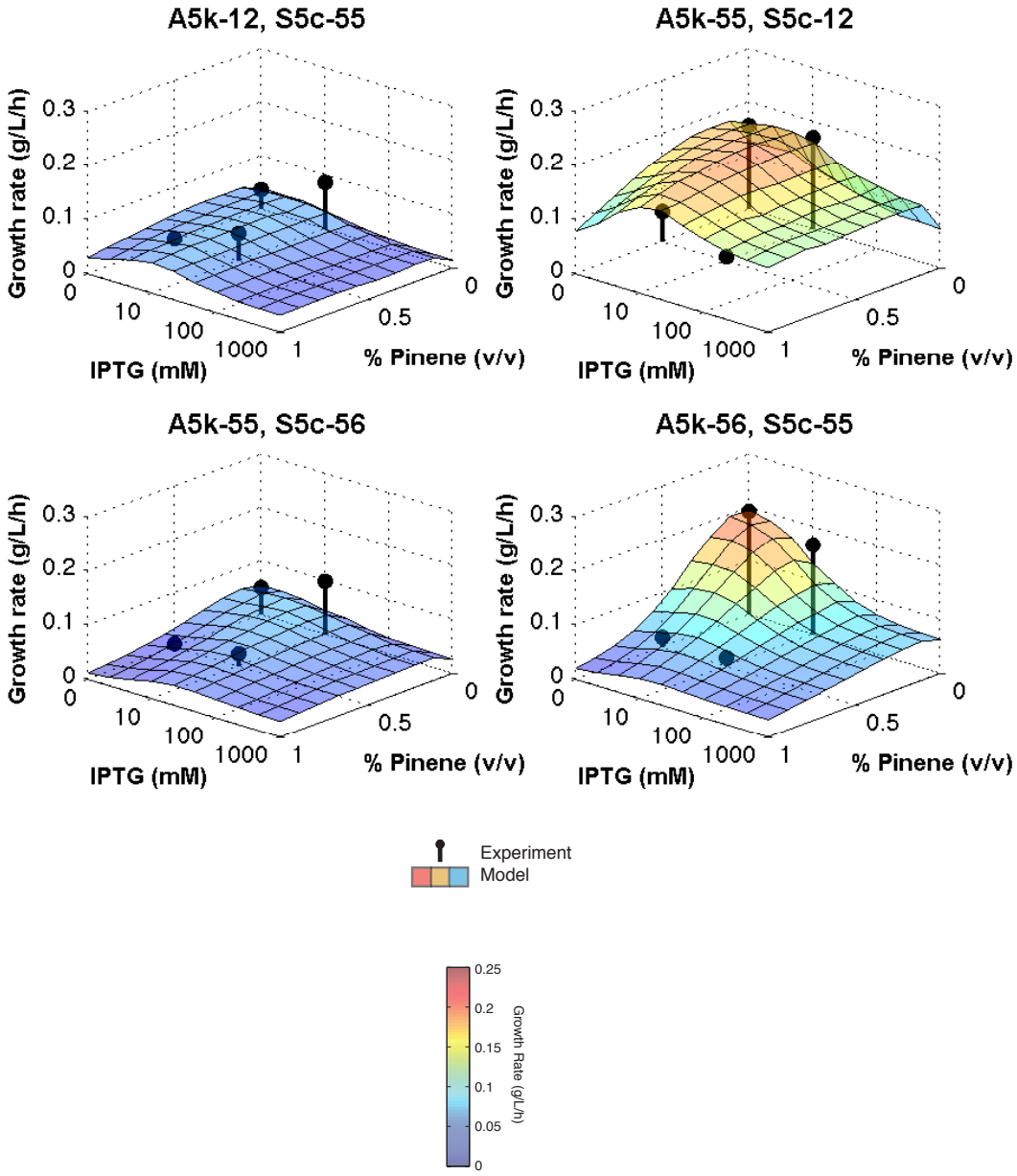

Figure 3.6: Toxicity profiles of four additional pump combinations tested. Black lines and dots represent experimentally measured growth rates and colored surfaces are modeling results.

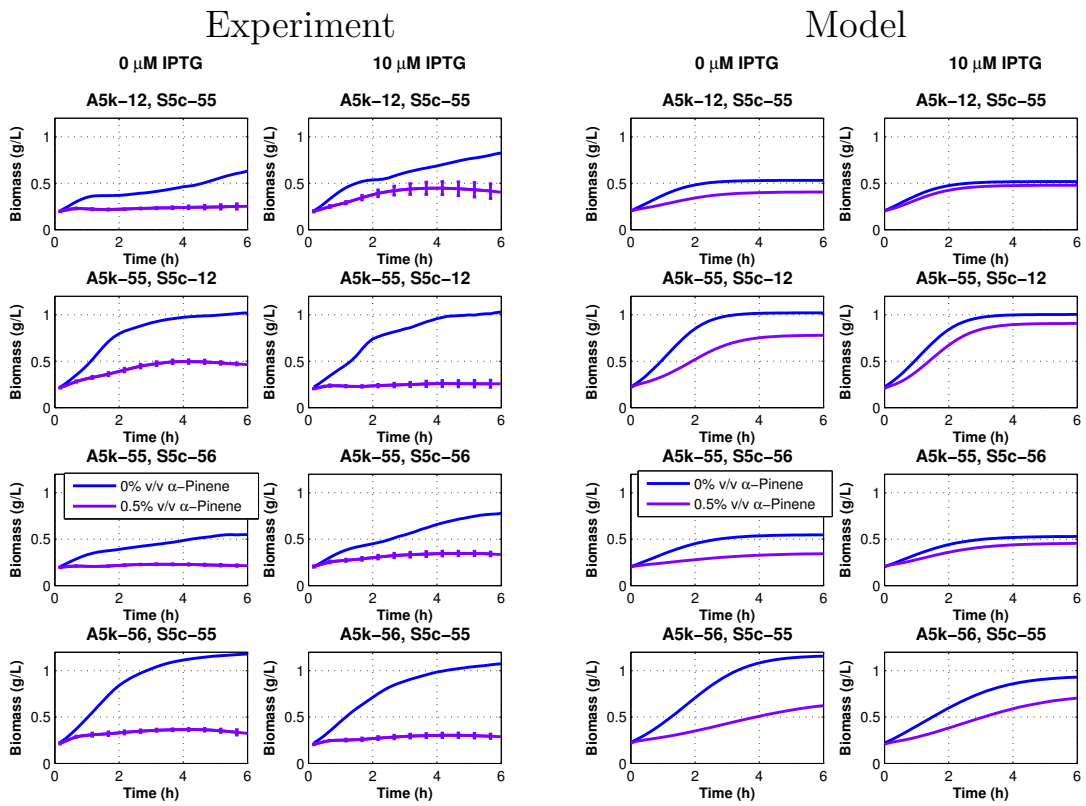

Figure 3.7: Growth curves of four additional pump combinations tested. (Left) Experimental data, error bars represent standard error for 3 biological replicates. (Right) Model generated growth curves for the same conditions. In each set of figures, the left column has 0 μM IPTG and the right column is with 10μM IPTG as indicated by the text directly above each column. The strain information is given in the titles.

Bibliography

[1] Dunlop, Mary J., Zain Y. Dossani, Heather L. Szmidt, Hou Cheng Chu, Taek Soon Lee, Jay D. Keasling, Masood Z. Hadi, and Aindrila Mukhopadhyay. Engineering microbial biofuel tolerance and export using efflux pumps. Molecular systems biology 7, no. 1. (2011).

[2] Huu, N. B., Denner, E. B., Ha, D. T., Wanner, G., and Stan-Lotter, H. Marinobacter aquaeolei sp. nov., a halophilic bacterium isolated from a Vietnamese oil-producing well. International journal of systematic bacteriology, 49(2), 367-375. (1999).

[3] Lee, Angela, Weimin Mao, Mark S. Warren, Anita Mistry, Kazuki Hoshino, Ryo Okumura, Hiroko Ishida, and Olga Lomovskaya. Interplay between efflux pumps may provide either additive or multiplicative effects on drug resistance. Journal of bacteriology 182, no. 11, 3142-3150. (2000).

[4] Lee, Taek Soon, Rachel A. Krupa, Fuzhong Zhang, Meghdad Hajimorad, William J. Holtz, Nilu Prasad, Sung Kuk Lee, and Jay D. Keasling. BglBrick vectors and datasheets: a synthetic biology platform for gene expression. Journal of biological engineering 5, no. 1: 1-14. (2011).

[5] Nelson, K. E., Weinel, C., Paulsen, I. T., Dodson, R. J., Hilbert, H., Martins dos Santos, V. A. P., Fouts, D. E., Gill, S. R., Pop, M., Holmes, M., Brinkac, L., Beanan, M., DeBoy, R. T., Daugherty, S., Kolonay, J., Madupu, R., Nelson, W., White, O., Peterson, J., Khouri, H., Hance, I., Lee, P. C., Holtzapple, E., Scanlan, D., Tran, K., Moazzez, A., Utterback, T., Rizzo, M., Lee, K., Kosack, D., Moestl, D., Wedler, H., Lauber, J., Stjepandic, D., Hoheisel, J., Straetz, M., Heim, S., Kiewitz, C., Eisen, J., Timmis, K. N., Düsterhöft, A., Tümmler, B. and Fraser, C. M.. Complete genome sequence and comparative analysis of the metabolically versatile Pseudomonas putida KT2440. Environmental Microbiology, 4: 799-808. (2002).

[6] Schneiker, S., dos Santos, V. A. M., Bartels, D., Bekel, T., Brecht, M., Buhrmester, J., and Golyshin, P. N.. Genome sequence of the ubiquitous hydrocarbon-degrading marine bacterium Alcanivorax borkumensis. Nature biotechnology, 24(8), 997-1004.(2006).

[7] Singer, E., Webb, E. A., Nelson, W. C., Heidelberg, J. F., Ivanova, N., Pati, A., and Edwards, K. J.. Genomic potential of Marinobacter aquaeolei, a biogeochemical ŇopportunitrophÓ. Applied and environmental microbiology, 77(8), 2763-2771. (2011).

[8] Yakimov, M. M., Golyshin, P. N., Lang, S., Moore, E. R., Abraham, W. R., Lünsdorf, H., and Timmis, K. N.. Alcanivorax borkumensis gen. nov., sp. nov., a new, hydrocarbon-degrading and surfactant-producing marine bacterium. International journal of systematic bacteriology, 48(2), 339-348. (1998).

3.3 Supplementary Information

3.3.1 Supplementary Tables

Table 3.2: Primers used in this study. Primers used to amplify plasmid vectors and efflux pump genes for the construction of strains used in this study are listed here with their nucleotide sequences. All primers were ordered from and synthesized by Thermo Fischer Scientific.

Name	**Description / Target**	**Sequence**
F-epl56-S5c	Insert epl56 forward	TTTAAGAAGGAGATATACATATG CAGACAGAGAAGAGTTT
R-epl56-S5c	Insert epl56 reverse	CCTTACTCGAGTTTGGATCCGTC AGTGTTTTCATAATCAG
R-pBbA5k-S5c	Vector pBbS5c-epl56 reverse	AAACTCTTCTCTGTCTGCATATG TATATCTCCTTCTTAAA
F-PbbA5k-S5c	Vector pBbS5c-epl56 forward	CTGATTATGAAAACACTGACGG ATCCAAACTCGAGTAAGG
F-seq-up	Sequencing primer for pBbS5c-epl_, forward	GGCACCCCAGGCTTTAC
R-seq-dn	Sequencing primer for pBbS5c-epl56, reverse	AGAGCGTTCACCGACAAAC
F-epl12-12	Insert epl12 forward	GATCTTTTAAGAAGGAGATATAC ATATGCCTACTACCCTCTCCC
R-epl12-12	Insert epl12 reverse	CCTTACTCGAGTTTGGATCCTC AGCTTTCGCGGGGCA
F-pBbS5c-12	Vector pBbS5c-epl12 froward	TGCCCCGCGAAAGCTGAGGATC CAAACTCGAGTAAGG
R-pBbS5c-12	Vector pBbS5c-epl12 reverse	GGGAGAGGGTAGTAGGCATATGT ATATCTCCTTCTTAAAAGATC
F-epl95-95	Insert epl95 forward	GATCTTTTAAGAAGGAGATATAC ATATGTATATACTGAACCTG ATTCA

Table 3.2 continued...

Name	**Description / Target**	**Sequence**
R-epl95-95	Insert epl95 reverse	CCTTACTCGAGTTTGGATCCTTA GCGGCTGGCCACAT
F-pBbS5c-95	Vector pBbS5c-epl95 forward	ATGTGGCCAGCCGCTAAGGATCC AAACTCGAGTAAGG
R-pBbS5c-95	Vector pBbS5c-epl95 reverse	TGAATCAGGTTCAGTATATACATA TGTATATCTCCTTCTTAAAAGATC
F-epl55-55	Insert epl55 forward	GATCTTTTAAGAAGGAGATATAC ATGTGATTTCAAACAAACACCT
R-epl55-55	Insert epl55 reverse	CTTACTCGAGTTTGGATCCTTA ATCGTCAGCGGATTT
F-pBbS5c-55	Vector pBbS5c-epl55 forward	AAATCCGCTGACGATTAAGGAT CCAAACTCGAGTAAG
R-pBbS5c-55	Vector pBbS5c-epl55 reverse	AGGTGTTTGTTTGAAATCACATG TATATCTCCTTCTTAAAAGATC
R-seq-12	Reverse sequencing primer for epl12 (Forward is same for all)	AGGGTTTCTACGCGCACTT
R-seq-55	Reverse sequencing primer for epl55	TTGTTCTTCCACTTCATACA
R-seq-95	Reverse sequencing primer for epl95	GAAACCGCTGCGCATAAT

Chapter 4

Ionic Liquid Tolerance Model

Portions of this chapter were published in the journal PLoS ONE on July 1, 2014 (1).

4.1 Background

In biofuel production, residual ionic liquids leftover from feedstock pretreatment can make it into the bioreactor, this inhibits the growth of the biofuel producing bacteria, reducing fuel yields. We will now apply these modeling techniques to experimental data for toxicity and export of ionic liquids. Previous studies have demonstrated that the efflux pump encoded by the gene *eilA* from *Enterobacter lignolyticus* can reduce the toxicity of residual ionic liquids in the reactor (2). In collaboration with researchers at the Joint Bio-Energy Institute (JBEI), we developed a mathematical model to explain experimental findings on ionic liquid toxicity (1). Our colleagues at JBEI have studied the effectiveness of this pump when expressed heterologously in *E. coli* under the control of both dynamic and constitutive promoters. Three dynamic controllers; P*marR*, P*ydfO*, and P*ydfA* were designed by selecting native *E. coli* promoters that were active in the presence of the ionic liquid $[C_2mim]Cl$. These were compared to the IPTG inducible constitutive promoter, P*lacUV5*, as well as a control strain with no promoter.

4.2 Modeling Methods

Equaitons 4.1- 4.5 were used to model cell growth, pump protein concentration, and toxicity due to ionic liquids. Each equation shows the time derivative of a state variable. N represents the biomass concentration in the control volume, S is the substrate concentration, P is the efflux pump concentration, and C_i is the intracellular ionic liquid concentraiton.

$$\dot{N} = \mu_{max} N \frac{S}{K_s + S} \frac{1}{1 + (\frac{C_i}{K_c})^h} \frac{1}{1 + \frac{P}{K_p}} \tag{4.1}$$

$$\dot{S} = -\frac{1}{\gamma} \mu_{max} N \frac{S}{K_S + S} \tag{4.2}$$

$$\dot{P} = \alpha_{P0} + \alpha_p - \beta P \tag{4.3}$$

$$\dot{P} = \alpha_{P0} + \alpha_p \frac{C_i}{C_i + \gamma_p} - \beta P \tag{4.4}$$

$$\dot{C_i} = \alpha_c 0 \frac{V_e}{V_i} (C_e - C_i) - C_i \alpha_c P \tag{4.5}$$

First, the parameters for growth without any ionic liquids were determined from the uninhibited and uninduced growth curve, μ_{max}, K_s, and γ. Figure 4.1 shows the experimental data for an uninhibited growth curve along with the simulation results. All parameter values are listed in the caption of the figure that they first appear in, and remain the same for all subsequent simulations in the current section unless otherwise mentioned. All constants in this section are also given in Table 4.1. Equation 4.1 is the modified Monod equation used to model ionic liquid inhibition and pump toxicity.

Next, the parameters for toxicity of the ionic liquid without the efflux pumps , K_c and h, and the toxicity of the efflux pump without any ionic liquid, K_p, were determined. Figure 4.2 shows the endpoints of experimental growth curves over a range of ionic liquid concentrations plotted along with the experimentally determined toxicity profile. The entire simulated growth curves along with their experimental analogs can be seen in the supplementary section of this chapter, Fig. 2.8. Overexpression of *eilA* proved to be minimally toxic (1) (Fig. 4.5). Protein levels were simulated using Equation 4.3 for the P*lacUV5* controller, and Equation 4.4 for the ionic liquid responsive dynamic controllers. The basal and maximum expression rates,α_{p0} and α_p, and thresholds, γ_p, of the

controllers were set based on protein measurements taken over a range of ionic liquid concentrations (1). For the promoterless case, α_p was set to zero. β accounts for pump protein dilution due to cell division.

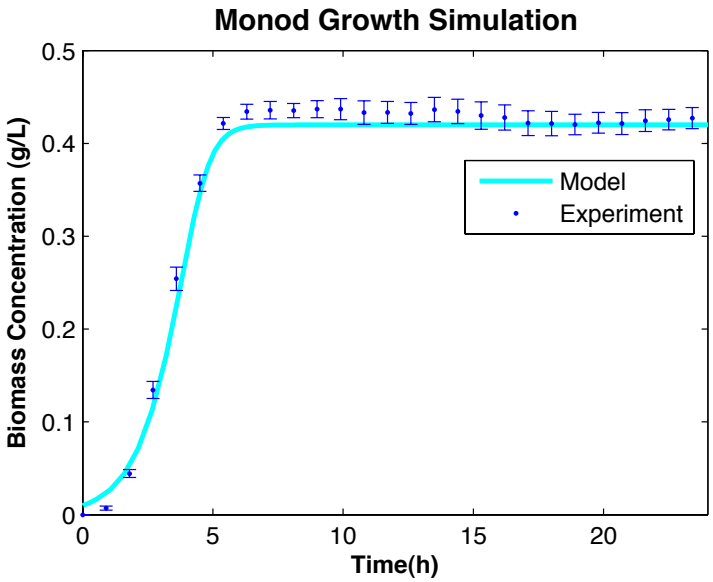

Figure 4.1: Simulated growth curve and experimental data for E. coli. Standard deviation indicated by error bars. Parameter values: $\mu_{max} = 1.71/h$, $K_s = 8g/L$, $\gamma = 0.041$. *Initial Conditions:* $N_0 = 0.01g/L$, $S_0 = 10g/L$ *glucose.*

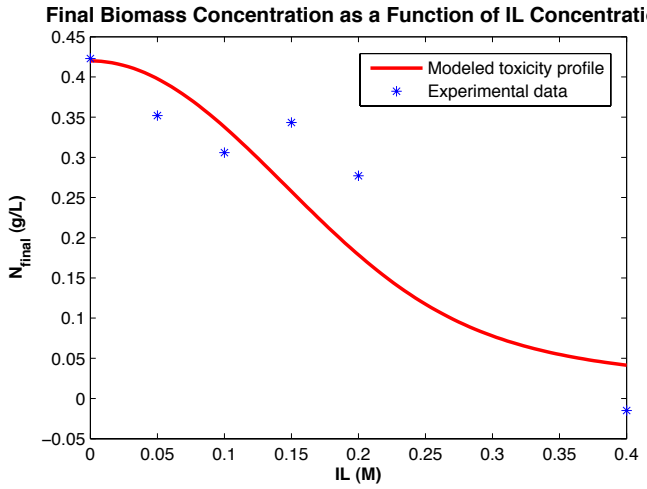

Figure 4.2: Toxicity profile for E. coli in the presence of $[C_2mim]Cl$ *without any efflux pump expression. Parameter values:* $K_c = 0.06g/L$, $h = 2$.

4.3 Results

Growth curves were modeled using the coupled set of differential equations consisting of Eqn. 4.1, Eqn. 4.2 along with Eqn. 4.3 or 4.4 (depending on controller type), and Eqn. 4.5. The rate of passive diffusion of ionic liquids across the membrane, $\alpha_c 0$, and the active export rate, α_c, were set to occur on physically realistic timescales and match the growth characteristics of the experimental data. Figure 4.3 shows the experimental results of each controller construct tested in *E. coli* over a range of ionic liquid concentrations. Figure 4.4 shows the corresponding simulation results. Additional results showing the temporal response of other state variables from this simulation can be found in the supplementary section of this chapter, Figs. 4.7 and 4.8.

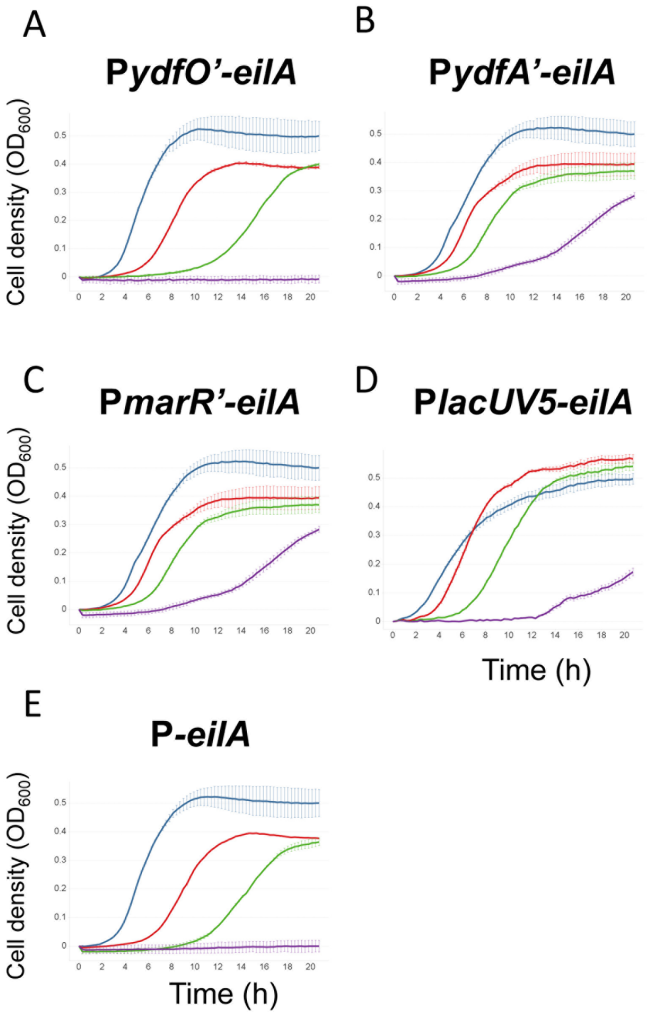

Figure 4.3: Performance of different eilA expression strains at increasing [C_2mim]Cl concentrations. Experimental data from collaborators at JBEI. Blue: 0 mM, red: 100 mM, green: 200 mM, purple: 400 mM [C_2mim]Cl.

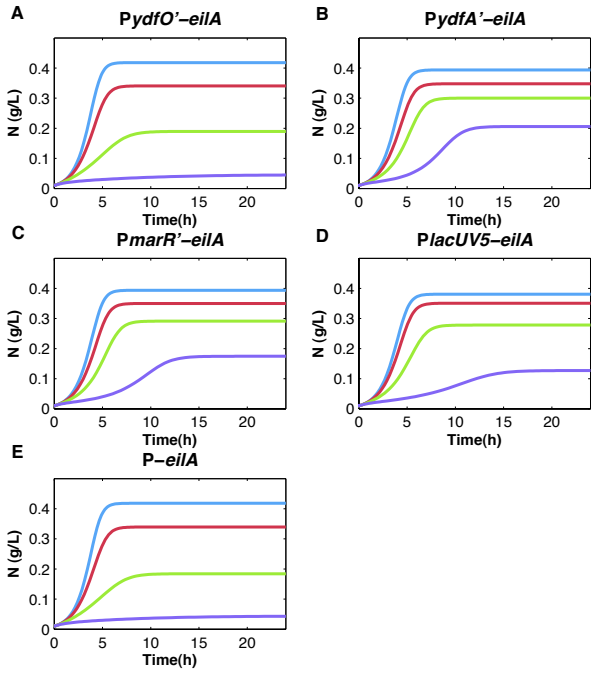

Figure 4.4: Modeling results comparing controllers at different $[C_2mim]Cl$ concentrations. Blue: 0 mM, red: 100 mM, green: 200 mM, purple: 400 mM $[C_2mim]Cl$. Parameters: $\beta = 1/h$, $\alpha_c 0 = 3.5(10^{-6})$, $\alpha_c = 0.75/h$.

The results indicate that the dynamic controllers perform at least as well as the IPTG inducible controller at high [C_2mim]Cl concentrations (400mM). This eliminates the need for using costly inducers in the biofuel production process. Also, at low concentrations of ionic liquid the dynamic controllers have an advantage because they are not expressing the pump gene unnecessarily. The relatively simple set of differential equations used in this model is able to capture the trends observed in the experimental data (Fig. 4.3 & 4.4). This means that despite the simplifications of the system assumed in the model, it can still be a useful tool for making predictions based on limited experimental data.

Bibliography

[1] Frederix, M., K. Hutter, J. Leu, T. S. Bath, W. J. Turner, T. L. Rüegg, H. W. Blanch, B. D. Simmons, P. D. Adams, J. D. Keasling, M. P. Thelen, M. J. Dunlop, C. J. Petzold, A. Mukhopadhyay. Development of a Native *Escherichia coli* Induction System for Ionic Liquid Tolerance. PloS one, 9(7), e101115. (2014).

[2] Rüegg, T. L., Kim, E. M., Simmons, B. A., Keasling, J. D., Singer, S. W., Lee, T. S., and Thelen, M. P. An auto-inducible mechanism for ionic liquid resistance in microbial biofuel production. Nature communications, 5. (2014).

4.4 Supplementary Information

4.4.1 Supplementary Tables

Table 4.1: Modeling constants for IL tolerance. All modeling constants used for the simulations in Chapter 4 are given here.

Symbol	**Value**	**Description**
μ_{max}	1.7/h	Maximum growth rate
h	2	Biofuel toxicity exponent, hill coefficient
γ	$0.041 g_{cells}/g_{substrate}$	Growth yield
K_s	8 g/L	Growth/substrate half saturation constant
K_c	0.06 M	IL toxicity half-saturation constant
K_p	3	pump toxicity half-saturation constant
α_{c0}	$3.5(10^{-6})$/h	Membrane permeability rate
α_c	0.75/h-M	IL export rate
α_{p0}	P*ydfO'-eilA*: 0.015/h P*ydfA'-eilA*: 0.22/h P*marR'-eilA*: .22/h P*lacUV5-eilA*: .06/h P-*eilA*: .014/h	Basal protein expression rate
α_p	P*ydfO'-eilA*: 0.015/h P*ydfA'-eilA*: 0.523/h P*marR'-eilA*: .34/h P*lacUV5-eilA*: .28/h	(Maximum) protein expression rate
γ_c	P*ydfO'-eilA*: 0.0075 M P*ydfA'-eilA*: 0.02 M P*marR'-eilA*: .02 M	Pump expression threshold
β	1/h	Pump protein degradation rate

4.4.2 Supplementary Figures

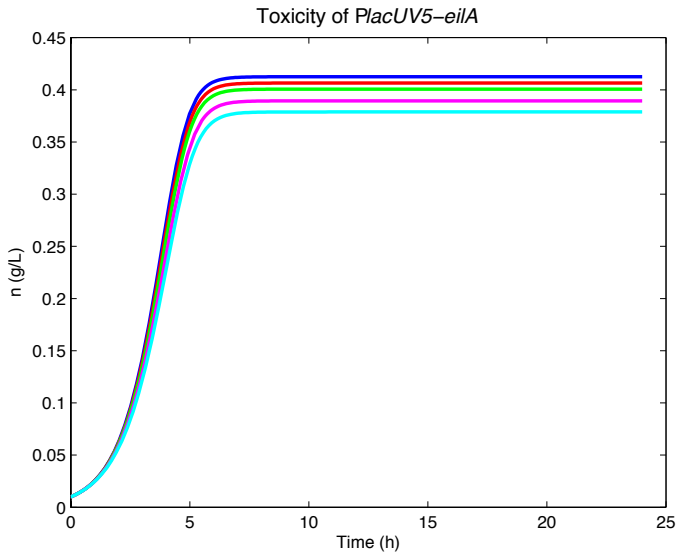

Figure 4.5: Pump toxicity of EilA. The ionic liquid exporting efflux pump -eilA (2) was determined experimentally to be minimally toxic. These are the simulation results used to determine the IL toxicity half saturation constant and Hill coefficient. The spread between curves was set to reproduce the experimental results in (1).

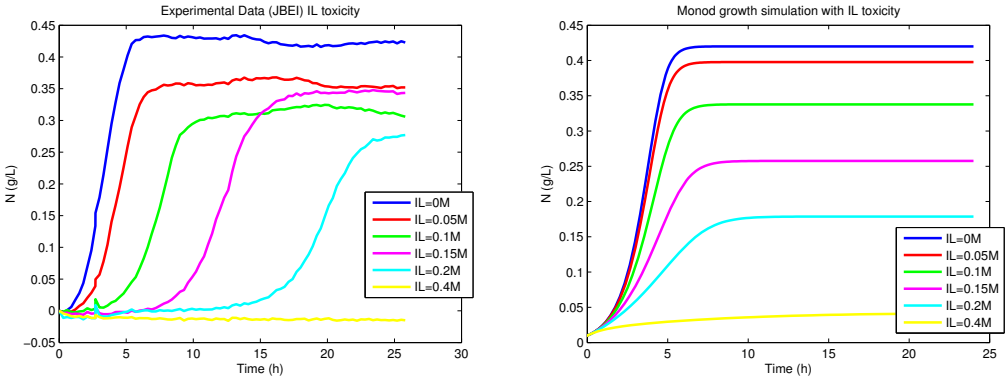

Figure 4.6: Toxicity of $[C_2mim]Cl$ to wildtype E. coli . (Left) Experimentally measured growth curves from (1). (Right) Simulated growth curves for the same conditions.

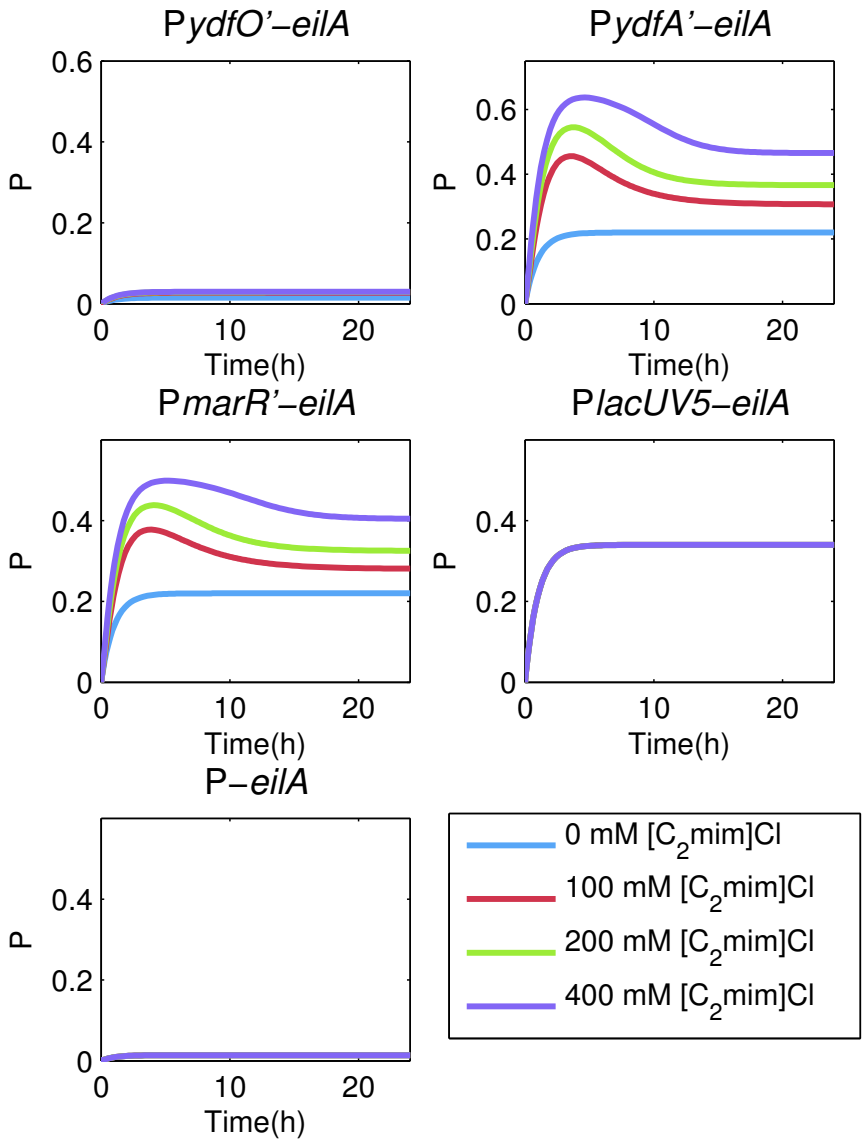

Figure 4.7: Simulated protein concentration curves for each controller in the study. The results shown here come from the same simulation used to produce Fig. 4.1. The basal and maximum rates of protein production were determined from proteomics data collected at JBEI (1).

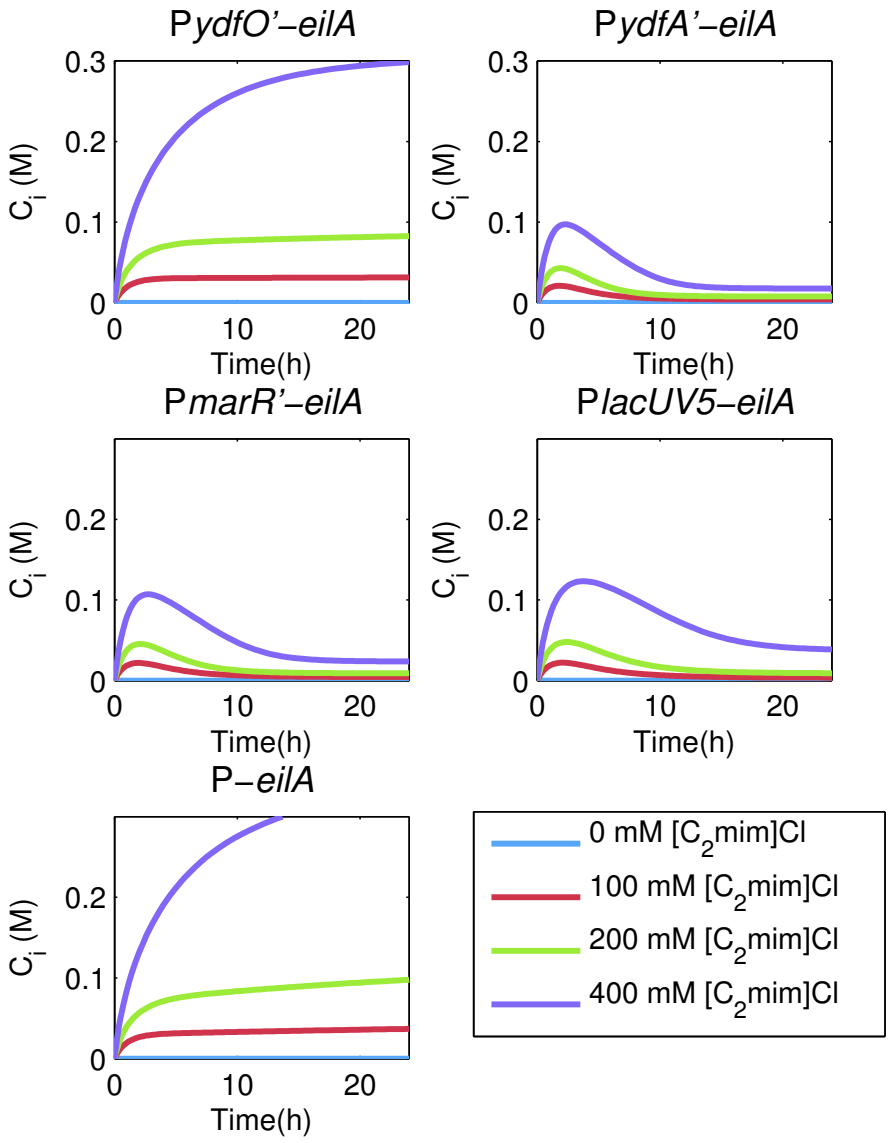

Figure 4.8: Simulated ionic liquid concentration curves for each controller in the study. The results shown here come from the same simulation used to produce Fig. 4.1 and Fig. 4.7. The legend indicates the concentration of ionic liquid in the entire reactor. Different promoter strengths and controller designs result in different amounts of reduction of intracellular ionic liquid.

Bibliography

[1] Frederix, M., K. Hutter, J. Leu, T. S. Bath, W. J. Turner, T. L. Rüegg, H. W. Blanch, B. D. Simmons, P. D. Adams, J. D. Keasling, M. P. Thelen, M. J. Dunlop, C. J. Petzold, A. Mukhopadhyay. Development of a Native *Escherichia coli* Induction System for Ionic Liquid Tolerance. PloS one, 9(7), e101115. (2014).

[2] Rüegg, T. L., Kim, E. M., Simmons, B. A., Keasling, J. D., Singer, S. W., Lee, T. S., & Thelen, M. P.. An auto-inducible mechanism for ionic liquid resistance in microbial biofuel production. Nature communications, 5. (2014).

Conclusion

In this thesis we have used engineering principles and synthetic biology lab techniques to improve our understanding of the function and modularity of efflux pumps in providing tolerance to biofuel production conditions. We have used this understanding to demonstrate that certain combinations of efflux pumps, even though they may come from completely different organisms, can demonstrate a cooperative effect on improving biofuel tolerance. This suggests functional similarities between efflux pumps spanning multiple species, and the potential for the different components of the RND efflux pumps to work together. For example, perhaps the inner and trans-membrane proteins from epl12 are able to bind to the outer membrane channel from epl56, which would account for the cooperative effect we observed and modeled.

We have shown that a relatively simple set of differential equations can be a useful tool for predicting the performance of efflux pumps. The model can be used to test out a variety of gene controller designs, as we demonstrated in the chapter on ionic liquid tolerance. The model can also be used to predict the performance of new combinations of efflux pumps. For example, we can clearly see in Figures 2.3c-d and 2.8 how the pinene tolerance and pump toxicities from the two pumps (epl12 & epl56) combine to improve the performance of the combination strain. Also, we demonstrated the ability of the model to predict the performance of uncharacterized combinations in Figure 2.4 when we were able to predict that the combination A-epl56, S-epl12 would outperform A-epl55, S-epl95 at 0.5% pinene despite having a slower growth rate in the absence of pinene. We have shown that deterministic modeling using differential equations is a valuable tool to be used alongside experimental techniques to reduce the number of experiments necessary and provide some physical and mathematical explanation of the biological system being studied.

The model described in this thesis is based on assumptions that were made to simplify the equations. For example, we reduce the multi-step transcription and translation of efflux pump genes into proteins and subsequent protein folding and embedding in the membrane into a single equation modeling pump protein concentration directly. The model could be improved by accounting for RNA production and membrane insertion. Moreover, all chemical concentrations in the model are assumed to be uniform throughout the intracellular or extracellular domains, we are effectively modeling the average across the entire populaiton. In actuality there would be cell to cell variations in both

chemical concentrations and growth rate. The model could be modified to include stochasticity of gene expression as well as individual cell growth dynamics by modeling each cell in the population individually.

Further experiments could be conducted to extend our understanding of efflux pump interactions. For example it would be interesting to isolate the genes for the individual components of the tripartite pumps and try different combinations of the components from various pumps and see which are responsible for the tolerance provided. Also, by using proteomics it would be possible to directly measure efflux pump concentration and dynamics. More freedom of expression levels could be provided by changing the low copy vector (pBbS5c) to a plasmid with a promoter that responds orthogonally to another inducer (other than IPTG). Then, by running growth assay experiments with gradients of both inducers and biofuel, the optimum expression rates of the pumps relative to one another could be determined. Once this optimum ratio has been determined, biofuel responsive promoters could be designed and used to control expression of each pump so that the pumps would only be activated in the presence of biofuel.

Bibliography

Atsumi, S., Hanai, T. and Liao, J. C. Non-fermentative pathways for synthesis of branched-chain higher alcohols as biofuels. Nature 451, 86 to 89. (2008).

Brennan, T. C. R., Turner, C. D., Krömer, J. O., and Nielsen, L. K. Alleviating monoterpene toxicity using a two-phase extractive fermentation for the bioproduction of jet fuel mixtures in Saccharomyces cerevisiae. Biotechnology and Bioengineering, 109(10), 2513 to 22. (2012).

Dahl, M. K., Msadek, T., Kunst, F., and Rapoport, G. The phosphorylation state of the DegU response regulator acts as a molecular switch allowing either degradative enzyme synthesis or expression of genetic competence in Bacillus subtilis. Journal of Biological Chemistry, 267(20), 14509-14514. (1992).

Deris, J. B., Kim, M., Zhang, Z., Okano, H., Hermsen, R., Groisman, A., and Hwa, T. The innate growth bistability and fitness landscapes of antibiotic-resistant bacteria. Science (New York, N.Y.), 342(6162). (2013).

Dunlop, Mary J., Jay D. Keasling, and Aindrila Mukhopadhyay. A model for improving microbial biofuel production using a synthetic feedback loop. Systems and synthetic biology 4.2, 95-104. (2010).

Dunlop, Mary J., Zain Y. Dossani, Heather L. Szmidt, Hou Cheng Chu, Taek Soon Lee, Jay D. Keasling, Masood Z. Hadi, and Aindrila Mukhopadhyay. Engineering microbial biofuel tolerance and export using efflux pumps. Molecular systems biology 7, no. 1 (2011).

Fargione, Joseph, Jason Hill, David Tilman, Stephen Polasky, and Peter Hawthorne. Land clearing and the biofuel carbon debt. Science 319, no. 5867, 1235-1238. (2008).

Fisher, M. A., Boyarskiy, S., Yamada, M. R., Kong, N., Bauer, S., and Tullman-Ercek, D.. Enhancing tolerance to short-chain alcohols by engineering the *Escherichia coli* AcrB efflux pump to secrete the non-native substrate n-butanol. ACS synthetic biology, 3(1), 30-40. (2013).

Frederix, M., K. Hutter, J. Leu, T. S. Bath, W. J. Turner, T. L. Rüegg, H. W. Blanch, B. D. Simmons, P. D. Adams, J. D. Keasling, M. P. Thelen, M. J. Dunlop, C. J. Petzold, A. Mukhopadhyay. Development of a Native *Escherichia coli* Induction System for Ionic Liquid Tolerance. PloS one, 9(7), e101115. (2014).

Gibson, D. G., Young, L., Chuang, R. Y., Venter, J. C., Hutchison, C. A., and Smith, H. O.. Enzymatic assembly of DNA molecules up to several hundred kilobases. Nature methods, 6(5), 343-345. (2009).

Neidhardt, F. Escherichia coli and Salmonella: Cellular and molecular biology. ASM Press. (1996).

Harrison, M. E., and Dunlop, M. J.. Synthetic feedback loop model for increasing microbial biofuel production using a biosensor. Frontiers in microbiology, 3. (2012).

Harvey, Benjamin G., Michael E. Wright, and Roxanne L. Quintana. High-density renewable fuels based on the selective dimerization of pinenes. Energy and Fuels 24.1, 267-273. (2009).

Huu, N. B., Denner, E. B., Ha, D. T., Wanner, G., and Stan-Lotter, H. Marinobacter aquaeolei sp. nov., a halophilic bacterium isolated from a Vietnamese oil-producing well. International journal of systematic bacteriology, 49(2), 367-375. (1999).

Lee, Taek Soon, Rachel A. Krupa, Fuzhong Zhang, Meghdad Hajimorad, William J. Holtz, Nilu Prasad, Sung Kuk Lee, and Jay D. Keasling. "BglBrick vectors and datasheets: a synthetic biology platform for gene expression." Journal of biological engineering 5(1), 1-14. (2011).

Lee, Angela, Weimin Mao, Mark S. Warren, Anita Mistry, Kazuki Hoshino, Ryo Okumura, Hiroko Ishida, and Olga Lomovskaya. Interplay between efflux pumps may provide either additive or multiplicative effects on drug resistance. Journal of bacteriology 182, no. 11, 3142-3150. (2000).

Jacques Monod. The growth of bacterial cultures. Annual Reviews in Microbiology. (1949).

Mora-Pale, Mauricio, Luciana Meli, Thomas V. Doherty, Robert J. Linhardt, and Jonathan S. Dordick. Room temperature ionic liquids as emerging solvents for the pretreatment of lignocellulosic biomass. Biotechnology and bioengineering 108(6), 1229-1245. (2011).

Nelson, K. E. and Weinel, C. and Paulsen, I. T. and Dodson, R. J. and Hilbert, H. and Martins dos Santos, V. A. P. and Fouts, D. E. and Gill, S. R. and Pop, M. and Holmes, M. and Brinkac, L. and Beanan, M. and DeBoy, R. T. and Daugherty, S. and Kolonay, J. and Madupu, R. and Nelson, W. and White, O. and Peterson, J. and Khouri, H. and Hance, I. and Lee, P. Chris and Holtzapple, E. and Scanlan, D. and Tran, K. and Moazzez, A. and Utterback, T. and Rizzo, M. and Lee, K. and Kosack, D. and Moestl, D. and Wedler, H. and Lauber, J. and Stjepandic, D. and Hoheisel, J. and Straetz, M. and Heim, S. and Kiewitz, C. and Eisen, J. and Timmis, K. N. and Düsterhöft, A. and Tümmler, B. and Fraser, C. M. Complete genome sequence and comparative analysis of the metabolically versatile Pseudomonas putida KT2440. Environmental Microbiology, 4(12), 799-808. (2002).

Nicolaou, S. a, Gaida, S. M., & Papoutsakis, E. T. A comparative view of metabolite and substrate stress and tolerance in microbial bioprocessing: From biofuels and chemicals, to biocatalysis and bioremediation. Metabolic Engineering, 12(4), 307 to 31. (2010).

Nikaido, Hiroshi. Multidrug efflux pumps of gram-negative bacteria. Journal of Bacteriology 178(20), 5853. (1996).

Olson, E. J., Hartsough, L. A., Landry, B. P., Shroff, R., & Tabor, J. J. Characterizing bacterial gene circuit dynamics with optically programmed gene expression signals. Nature methods. (2014).

Paulsen, Ian T. Multidrug efflux pumps and resistance: regulation and evolution. Current opinion in microbiology 6.5, 446-451. (2003).

Peralta-Yahya, Pamela P., Fuzhong Zhang, Stephen B. Del Cardayre, and Jay D. Keasling. Microbial engineering for the production of advanced biofuels. Nature 488, no. 7411, 320-328. (2012).

Phillips, R., Kondev, J., Theriot, J., and Garcia, H.. Physical biology of the cell (pp. 281-321). New York: Garland Science. (2009).

Piddock, L. J. Clinically relevant chromosomally encoded multidrug resistance efflux pumps in bacteria. Clinical microbiology reviews, 19(2), 382-402. (2006).

Ramos, Juan L., Estrella Duque, MaríaTrinidad Gallegos, Patricia Godoy, María Isabel Ramos-González, Antonia Rojas, Wilson Terán, and Ana Segura. Mechanisms of solvent tolerance in gram-negative bacteria. Annual Reviews in Microbiology 56, no. 1, 743 to 768. (2002).

Rojas, Antonia, Estrella Duque, Gilberto Mosqueda, Geir Golden, Ana Hurtado, Juan L. Ramos, and Ana Segura. Three Efflux Pumps Are Required To Provide Efficient Tolerance to Toluene in Pseudomonas putidaDOT-T1E. Journal of bacteriology 183, no. 13: 3967-3973. (2001).

Rosner, Judah L., and Robert G. Martin. Reduction of Cellular Stress by TolC- Dependent Efflux Pumps in Escherichia coli Indicated by BaeSR and CpxARP Activation of spy in Efflux Mutants. Journal of bacteriology 195.5, 1042-1050. (2013).

Rüegg, T. L., Kim, E. M., Simmons, B. A., Keasling, J. D., Singer, S. W., Lee, T. S., & Thelen, M. P. An auto-inducible mechanism for ionic liquid resistance in microbial biofuel production. Nature communications, 5. (2014).

Sarria, S., Wong, B., Martín, H. G., Keasling, J. D., and Peralta-Yahya, P.. Microbial Synthesis of Pinene. ACS Synthetic Biology. (2014).

Schneiker, S., dos Santos, V. A. M., Bartels, D., Bekel, T., Brecht, M., Buhrmester, J., and Golyshin, P. N.. Genome sequence of the ubiquitous hydrocarbon-degrading marine bacterium Alcanivorax borkumensis. Nature biotechnology, 24(8), 997-1004.(2006).

Singer, E., Webb, E. A., Nelson, W. C., Heidelberg, J. F., Ivanova, N., Pati, A., and Edwards, K. J.. Genomic potential of Marinobacter aquaeolei, a biogeochemical ŇopportunitrophÓ. Applied and environmental microbiology, 77(8), 2763-2771. (2011).

Wagner, S., Baars, L., Ytterberg, a J., Klussmeier, A., Wagner, C. S., Nord, O., de Gier, J.W.. Consequences of membrane protein overexpression in Escherichia coli. Molecular & Cellular Proteomics : MCP, 6(9), 1527-50. (2007).

Wagner, S., Klepsch, M. M., Schlegel, S., Appel, A., Draheim, R., Tarry, M., and de Gier, J. W.. Tuning Escherichia coli for membrane protein overexpression. Proceedings of the National Academy of Sciences, 105(38), 14371-14376. (2008).

Wood, K. B., and Cluzel, P.. Trade-offs between drug toxicity and benefit in the multi-antibiotic resistance system underlie optimal growth of E . coli. (2012).

Yakimov, M. M., Golyshin, P. N., Lang, S., Moore, E. R., Abraham, W. R., Lünsdorf, H., and Timmis, K. N.. Alcanivorax borkumensis gen. nov., sp. nov., a new, hydrocarbon-degrading and surfactant-producing marine bacterium. International journal of systematic bacteriology, 48(2), 339-348. (1998).

Yang, Jianming, Qingjuan Nie, Meng Ren, Hongru Feng, Xinglin Jiang, Yanning Zheng, Min Liu, Haibo Zhang, and Mo Xian. "Metabolic engineering of Escherichia coli for the biosynthesis of alpha-pinene." Biotechnol Biofuels 6: 60. (2013).

Zgurskaya, H. I., Krishnamoorthy, G., Ntreh, A., and Lu, S.. Mechanism and function of the outer membrane channel TolC in multidrug resistance and physiology of enterobacteria. Frontiers in microbiology, 2. (2011).

Zhang, F., Carothers, J. M., and Keasling, J. D.. Design of a dynamic sensor-regulator system for production of chemicals and fuels derived from fatty acids. Nature biotechnology, 30(4), 354-359. (2012).